Oceanological and Hydrobiological Studies

International Journal of Oceanography and Hydrobiology

Volume 55, No. 2 June 2026
pages (169-206)

ISSN 1730-413X
eISSN 1897-3191

Modeling of *Eucheuma cottonii* habitat suitability in relation to upwelling and the Indian Ocean Dipole in Cilacap and Kebumen Coastal Waters, Indonesia

by

Dwi Sunu Widyartini[1],
Ibrahim Kholilullah[2,*,a]

DOI: **https://doi.org/10.26881/oahs-2026.1.12**
Category: **Original research papers**
Received: **February 03, 2026**
Accepted: **April 22, 2026**

[1]*Biology Faculty, Jenderal Soedirman University, Purwokerto, Indonesia*
[2]*Marine Science and Technology Department, Bogor Agricultural University: Institut Pertanian Bogor, Bogor, Indonesia*

[a]*(https://orcid.org/0000-0001-9106-3389)*

Abstract

This study examines the influence of climate variability associated with the Indian Ocean Dipole (IOD) on the habitat suitability of *E. cottonii* cultivation in the coastal waters of Cilacap and Kebumen, southern Java. A Habitat Suitability Index (HSI) model was developed using a Boolean threshold implemented in Python. Environmental parameters included sea surface temperature (SST), salinity, nitrate concentration, surface current velocity, and bathymetry. The analysis focused on three representative years reflecting different climate conditions: negative IOD (2016), normal conditions (2018), and positive IOD (2019) from June–September. Results indicate that seasonal upwelling in southern Java tends to reduce habitat suitability for *E. cottonii*. During normal and positive IOD conditions, stronger upwelling from July to September corresponded with lower HSI values compared with June. In contrast, during the negative IOD phase, when upwelling signals were weaker, HSI values remained relatively stable. Kruskal–Wallis results indicate significant differences in SST, salinity, and nitrate among climate conditions, whereas surface currents show no significant variation. Sensitivity analysis suggests that bathymetry contributes more strongly to habitat suitability, while other parameters vary under different IOD conditions. Because the analysis is based on only three representative years, the results should be interpreted as exploratory rather than a generalized climatic pattern.

Key words: Indian Ocean Dipole, *Eucheuma cottonii*, upwelling, habitat suitability, modeling

* Corresponding author: *kholilullahibrahim@gmail.com*

Highlights

- This study examines the influence of the Indian Ocean Dipole (IOD) on the habitat suitability of *Eucheuma cottonii* in the coastal waters of Cilacap and Kebumen, which represents the novelty and main objective of this research.
- Results indicate that seasonal upwelling in southern Java tends to reduce habitat suitability for *E. cottonii*.
- During normal and positive IOD conditions, stronger upwelling from July to September corresponded with lower Habitat Suitability Index (HSI) values compared with June. In contrast, during the negative IOD phase, when upwelling signals were weaker, HSI values remained relatively stable.
- The Kruskal–Wallis test analysis showed significant differences in sea surface temperature (SST), salinity, and nitrate among climate conditions, whereas surface current velocity did not exhibit significant interannual variation.
- The combination of sensitivity map analysis and parameter contribution values indicates suggests that bathymetry (water depth) may play a relatively important role in shaping habitat suitability patterns, while other oceanographic parameters (SST, salinity, nitrate, and surface current velocity) function as dynamic variables whose influence may vary depending on the prevailing IOD climate conditions.

1. Introduction

E. cottonii is one of the major seaweed commodities cultivated in Indonesia (Manurung et al., 2021; Wahyuni et al., 2023; Wijayanto et al., 2020). The economic benefits obtained from its cultivation can reach IDR 19,500,000 (US$1184.59) per cultivated area or IDR 23,900,000 (US$1451.88) per hectare per harvest season (Wahyuni et al., 2023), with a cultivation period ranging from 30 to 65 days (Wijayanto et al., 2020). The success of seaweed cultivation is strongly influenced by site selection (Casadebaig et al., 2022) therefore, identifying suitable cultivation areas is crucial. One rapidly developing approach for this purpose is habitat suitability modeling (Bertelli et al., 2022; Stephenson et al., 2021; Stuart et al., 2021). Habitat suitability in coastal waters is largely affected by climate variability and oceanographic factors (Gokturk et al., 2022; Sun et al., 2024).

The coastal upwelling system along the southern coast of Java plays a significant role in determining marine productivity and controlling oceanographic conditions in the region (Napitupulu, 2025; Rochmatika & Bahtiar, 2023). In general, upwelling is defined as the upward movement of subsurface waters to the surface, driven by Ekman pumping resulting from persistent wind forcing and the Coriolis effect (Koropitan et al., 2021). In addition to the influence of the southeast monsoon, coastal upwelling along southern Java is frequently modulated by large-scale climate phenomena such as the El Niño–southern oscillation (ENSO) and the Indian Ocean Dipole (IOD) (Widagdo et al., 2025), which can either intensify or weaken the upwelling system (Hafiz et al., 2024; Oktaviani et al., 2021). Consequently, the coastal waters of Cilacap and Kebumen, as part of the southern Java upwelling system, are directly affected by these climate phenomena.

Coastal upwelling along southern Java typically occurs during the peak of the southeast monsoon between June and September (JJAS) (Budiman et al., 2022; Horii et al., 2023; Koropitan et al., 2021). The IOD index data obtained from the Bureau of Meteorology (BOM) indicate that positive IOD conditions occurred during JJAS in 2019, negative IOD conditions occurred during JJAS in 2016, while 2018 can be classified as a normal year during the same period.

The IOD is a climate phenomenon characterized by anomalous cooling or warming of sea surface temperature (SST) in the eastern or western Indian Ocean. A positive IOD event occurs when SST in the eastern Indian Ocean (western Sumatra and Java) cools while SST in the western Indian Ocean (eastern Africa) warms, whereas the opposite pattern characterizes negative IOD events (Koropitan et al., 2021; Wang et al., 2024). This near-consecutive interannual climate variability (positive IOD in 2019, negative IOD in 2016, and normal conditions in 2018) provides a valuable opportunity to investigate the habitat suitability of *E. cottonii* in relation to upwelling dynamics and IOD variability in the coastal waters of Cilacap and Kebumen, Indonesia.

One approach that can be applied to address this issue is habitat suitability modeling. Several studies have linked habitat suitability modeling with IOD variability. Lan et al. (2013) examined the habitat suitability of yellowfin tuna (*Thunnus albacares*) in the western Indian Ocean and reported a significant increase in habitat suitability during negative IOD events and a decrease during positive IOD events. Lan et al. (2015) investigated the habitat suitability of swordfish (*Xiphias gladius*) in the Indian Ocean, showing significant increases along the northwestern Indian Ocean coast during positive IOD events and in the southern Indian Ocean during negative IOD events.

Koropitan et al. (2021) analyzed the habitat suitability of mackerel tuna (*Euthynnus affinis*) influenced by negative IOD conditions along the southern Java coast and found a significant decline in habitat suitability during negative IOD events. Wen et al. (2025) studied the habitat suitability of squid (*Sthenoteuthis oualaniensis*) in the northern Indian Ocean and demonstrated that suitable habitat areas were smaller during positive IOD events and larger during negative IOD events. To date, no studies have explicitly modeled seaweed aquaculture habitat suitability while simultaneously examining the influence of the IOD.

A review of the literature over the past decade indicates that most habitat suitability studies of *E. cottonii* remain largely static, typically conducted for a single time period and without integrating physical oceanographic dynamics or regional climate variability. Examples include studies conducted in Mandar Bay, West Sulawesi by Rusdi (2018); Tidung Island by Utama and Handayani (2018); the eastern coast of Tarakan Island by Lestari et al. (2019); Pasiea District, North Buton by Salihin et al. (2019); Parepare Bay by Damis and Saenong (2020); Ambon Baguala Bay by Lase et al. (2020); Sarawandori Bay, Yapen Papua by Numberi et al. (2020); West Sorkam, Central Tapanuli by Manurung et al. (2021); Takalar Lama by St Madina et al. (2022); Majene waters by Arbit et al. (2024); and Lapang Island waters by Wabang and Plaimo (2024). Most of these studies primarily focused on mapping habitat suitability based on local environmental parameters without linking them to larger-scale oceanographic forcing mechanisms.

To date, only Lestari et al. (2019) have related *E. cottonii* habitat suitability to climate variability associated with the ENSO, demonstrating that the potential cultivation area was larger during La Niña compared to El Niño conditions. However, the influence of major oceanographic processes such as coastal upwelling and the role of variability associated with the IOD on *E. cottonii* habitat suitability has not yet been explicitly investigated, particularly in the southern coastal waters of Java, a region known for its strong seasonal upwelling dynamics.

The main novelty of this study lies in integrating upwelling processes and IOD variability into the habitat suitability analysis of *E. cottonii*. This approach not only describes the spatial patterns of habitat suitability but also explains the oceanographic and climatic mechanisms that control its variability. This study represents the first attempt to explicitly assess the combined influence of upwelling and the IOD on *E. cottonii* habitat suitability in the coastal waters of Cilacap and Kebumen. The findings are expected to provide a stronger scientific basis for climate-adaptive seaweed aquaculture management and contribute to advancing theoretical understanding of how IOD-related climate variability influences coastal aquaculture environments.

2. Materials and methods

2.1. Study area

This study was conducted in the coastal waters of Cilacap and Kebumen, Indonesia, located between 108.5°E–109.8°E and 7.3°S–8.0°S (Figure 1).

2.2. Data

Environmental parameters included SST, salinity, surface current velocity (zonal [u] and meridional [v]), and nitrate concentration. Oceanographic data were obtained from the Copernicus Marine

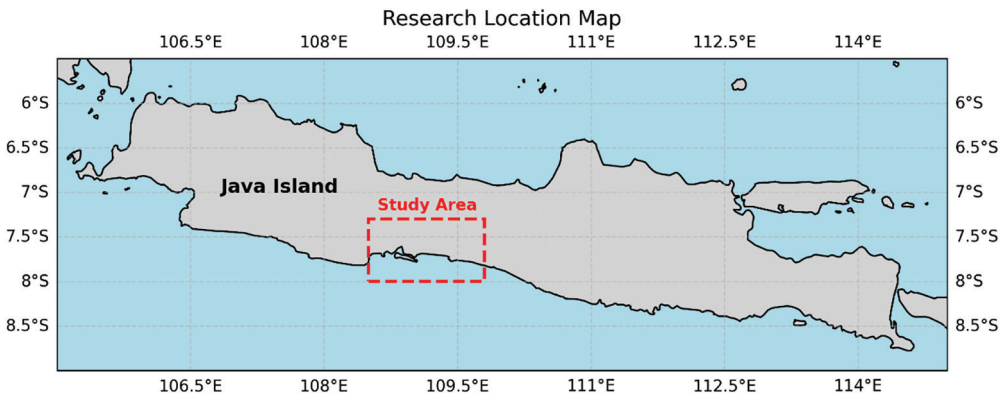

Figure 1

Study area map.

Service reanalysis products. SST, salinity, and surface current velocity were derived from the product GLOBAL_MULTIYEAR_PHY_001_030, which has a spatial resolution of 0.083° × 0.083°. Nitrate concentration data were obtained from the product GLOBAL_ANALYSISFORECAST_BGC_001_028, which has a spatial resolution of 0.25° × 0.25°. Both datasets provide monthly averaged fields that have undergone operational quality control and data assimilation procedures. Bathymetric data were obtained from the General Bathymetric Chart of the Oceans (GEBCO) dataset, specifically the GEBCO 2025 Grid. The bathymetric dataset has a spatial resolution of 0.0041667° × 0.0041667° (equivalent to 15″ or approximately 450 m at the equator). The analysis focused on the JJAS period to represent three contrasting climate conditions: negative IOD (2016), normal conditions (2018), and positive IOD (2019). Seasonal means were calculated as the arithmetic average of the monthly values during the JJAS period. All datasets were processed in NetCDF format.

Oceanographic variables from Copernicus Marine Service are operationally validated through the integration of numerical models, satellite observations, and in situ measurements. Given the quality control procedures implemented by the data provider, additional independent validation was not performed in this study. Nevertheless, the interpretation of results considers the spatial resolution limitations of the datasets (approximately 0.083°–0.25°), particularly in complex coastal environments. The GEBCO bathymetry grid represents a global compilation derived from hydrographic surveys and satellite altimetry and has undergone international quality control procedures. In this study, bathymetric data were primarily used as a depth constraint for habitat suitability filtering rather than for detailed seafloor morphology analysis; therefore, additional field validation was not conducted. However, it is acknowledged that local bathymetric accuracy may vary depending on the density of surveys in specific regions.

2.3. Model development

A habitat suitability analysis model for *E. cottonii* aquaculture was developed using a Boolean threshold approach within a geographic information system (GIS) framework and implemented using the Python programming language. The Boolean method assigns a score of 1 to environmental parameters that fall within suitable ranges and a score of 0 to those that fall outside suitable ranges (Ukhti et al., 2021). The suitability thresholds for *E. cottonii* cultivation, based on Manurung et al. (2021), were defined as follows: SST of 26°C–33°C, salinity of 25–35 PSU, nitrate concentration of 0.1–4.4 mg L^{-1} (equivalent to 1.61–70.96 mmol m^{-3}), current velocity of 0.1–0.4 m s^{-1}, and bathymetry (water depth) of 0.3–10 m. After scoring each parameter, the Habitat Suitability Index (HSI) was calculated using the Arithmetic Mean Model (AMM) (Wen et al., 2025), expressed as:

$$\mathrm{HSI} = \frac{1}{n}\left(S_{i1} + S_{i2} + S_{i3} + \ldots + S_{in}\right)$$

$$\mathrm{HSI} = \frac{1}{5}\left(S_{\mathrm{SST}} + S_{\mathrm{Salinity}} + S_{\mathrm{Nitrate}} + S_{\mathrm{Current}} + S_{\mathrm{Depth}}\right)$$

where:
HSI = Habitat Suitability Index.
S_i = suitability score for the ith parameter.
n = number of parameters.

This approach does not assume that all environmental parameters exert identical biological effects. Instead, it aims to avoid assigning subjective parameter weights when quantitative information regarding the relative contribution of each variable is not available. Previous studies indicate that the most influential environmental parameters affecting the growth of *E. cottonii* vary across locations. For instance, Manurung et al. (2021) identified current velocity as the dominant factor, whereas Numberi et al. (2020) emphasized water transparency as the primary parameter, and Lestari et al. (2019) highlighted the importance of dissolved oxygen (DO). Other studies suggest that multiple parameters may act simultaneously. Utama and Handayani (2018) reported substrate type, current velocity, and salinity as key factors; Wabang and Plaimo (2024) emphasized substrate, wave exposure, currents, water clarity, and depth; Arbit et al. (2024) identified temperature, salinity, and nutrients (nitrate and phosphate) as influential variables; while Salihin et al. (2019) underlined the role of salinity, transparency, phosphate, and nitrate. The variability of these findings indicates that no single environmental parameter consistently dominates across regions. Consequently, assigning differential weights without local biological evidence may introduce subjective bias. Therefore, equal weighting through a Boolean approach was adopted as a conservative and transparent strategy, allowing all ecologically relevant parameters to contribute equally to the habitat suitability assessment.

The compensatory assumption embedded in this model reflects the ecological tolerance range of *E. cottonii*, whereby suboptimal conditions in one parameter may still be compensated by favorable

conditions in others, provided that ecological thresholds are not exceeded. This approach is appropriate for studies aiming to explore spatial patterns of habitat suitability rather than to quantitatively predict aquaculture production. Under conditions of limited aquaculture production data, the Boolean approach combined with arithmetic averaging provides a reproducible method with minimal subjective assumptions and is supported by the empirical variability reported in previous studies.

All analyses were conducted using the Python programming language with the primary libraries xarray, numpy, scipy, matplotlib, and cartopy. The Python scripts used in this study are provided as Supplementary Material to ensure analytical reproducibility.

2.3.1. Pre-processing stage

The pre-processing stage began by loading each dataset using xarray.open_dataset() function and extracting the relevant variables. For variables containing a depth dimension, only the surface layer (depth = 0 m) was selected using the isel (depth = 0) function, as the study focuses on habitat suitability for seaweed cultivation in the upper water column. All variables were subsequently aligned to the spatial grid and temporal dimension of SST as the reference dataset using the interp_like() interpolation method with a nearest-neighbor approach. This procedure ensures spatial and temporal consistency among all environmental parameters prior to further analysis. Bathymetric data were also interpolated to the SST grid using the same method to ensure identical coordinate systems and spatial resolution across all layers. Surface current velocity was calculated from the zonal and meridional current components using the equation:

$$\sqrt{u^2 + v^2}$$

where:

u = represents the zonal current component and

v = represents the meridional current component.

2.3.2. Processing stage

A threshold-based suitability selection was then applied to each environmental parameter using ecological thresholds derived from previous literature: SST (26°C–33°C), salinity (25–35 PSU), nitrate (1.61–70.96 mmol m^{-3}), current velocity (0.1–0.4 m s^{-1}), and water depth (0.3–10 m). Each parameter was converted into a binary suitability score (0 = unsuitable; 1 = suitable). The final suitability score was calculated as the arithmetic mean of the five parameters, resulting in a HSI ranging from 0 to 1. To reduce spatial noise caused by grid discretization, Gaussian smoothing was applied using the gaussian_filter function with a sigma value of 1. The resulting suitability map was then spatially cropped to the study area covering the coastal waters of Cilacap and Kebumen (108.5°E–109.8°E; 8.0°S –7.3°S) using coordinate-based slicing. The analyzed coastal grid cells implicitly represent marine pixels that satisfy the depth criterion and contain valid values for all environmental parameters after interpolation and masking procedures. Spatial visualization was produced using the Plate Carrée projection through the cartopy library, and all outputs were exported as raster images (.png) for each analyzed month.

2.3.3. Model limitation

Although the physical datasets from the Copernicus Marine Service and bathymetric data from the GEBCO have undergone operational validation and therefore do not require additional independent validation, the HSI model developed in this study has not been validated against in situ observations or actual seaweed aquaculture production data. Therefore, the results represent potential habitat suitability based on biophysical conditions rather than empirical validation of cultivation performance in the field. This limitation is explicitly acknowledged and highlights the need for future studies integrating field survey data or aquaculture production records to improve the predictive accuracy of habitat suitability models.

2.4. Kruskal–Wallis test analysis

Differences in environmental parameters (SST, salinity, nitrate concentration, and surface current velocity) among climate conditions (negative IOD in 2016, neutral conditions in 2018, and positive IOD in 2019) during the JJAS period were evaluated using a non-parametric statistical approach. The analyzed data represent the midpoint values of each parameter within the study area for each month during JJAS, such that each climate condition is represented by four monthly observations. Initial visualization was performed using boxplots to illustrate the median, interquartile range (IQR), and variability among climate groups. Given the limited sample size, individual data points were overlaid on the boxplots using scatter markers to enhance transparency of the underlying data distribution. All visualizations were generated using the Matplotlib library in Python.

Hypothesis testing was conducted using the Kruskal–Wallis test, implemented through the kruskal function in the SciPy statistical module. This test was selected because of the relatively small sample size and its ability to compare multiple independent groups without assuming normal data distribution or homogeneity of variance. The Kruskal–Wallis test is a rank-based method that evaluates whether the medians of more than two independent groups differ significantly. The test statistic is expressed as the H value, with statistical significance evaluated at $\alpha = 0.05$. A *p*-value below 0.05 was interpreted as evidence of a statistically significant difference in parameter distributions among climate conditions. Because the analysis is based on spatially aggregated midpoint values and a limited temporal sample, statistical outcomes were interpreted cautiously as exploratory comparative evidence rather than causal inference. All analyses were performed using Python, and the complete scripts are provided as supplementary material to ensure transparency and reproducibility of the study.

2.5. Habitat model sensitivity analysis

Sensitivity analysis was conducted to evaluate the influence of each environmental parameter on the developed HSI model. This analysis is important in habitat modeling because the results of habitat suitability models can be influenced by the quality of input data, the selection of environmental variables, and the configuration of the model used. Therefore, sensitivity evaluation is necessary to ensure that the model produces stable and reliable habitat estimates (Arsenault et al., 2025). In this study, the sensitivity analysis was performed using a leave-one-parameter-out approach, also known as jackknife sensitivity analysis. This approach is widely used in species distribution and habitat modeling studies to identify environmental variables that have the strongest influence on model outcomes. The principle of this method is to recalculate the model output after removing one environmental parameter and then compare the resulting model output with the original model that includes all parameters (Wan et al., 2024).

The first step was to calculate the full HSI using all environmental parameters included in the model, namely SST, salinity, nitrate, current velocity, and bathymetry (water depth). The model was then recalculated by removing one environmental parameter at each iteration, producing an HSI value without the *i*-th parameter. The change in the habitat suitability index resulting from the removal of each parameter was calculated as the sensitivity value using the following equation:

$$\text{Sensitivity}_i = \text{HSI}_{\text{full}} - \text{HSI}_{(-i)}$$

where:

HSI_{full} = the habitat suitability index calculated using all environmental parameters

$\text{HSI}_{(-i)}$ = the habitat suitability index calculated after the *i*-th parameter is removed from the model.

This sensitivity value represents the magnitude of change in the model when a particular parameter is excluded from the HSI calculation. A larger change indicates a stronger influence of that parameter on the habitat suitability model. In addition, the relative contribution of each parameter to the model was calculated using the following equation:

$$\text{Contribution}_i = \frac{\text{HSI}_{\text{full}} - \text{HSI}_{(-i)}}{\text{HSI}_{\text{full}}}$$

The relative contribution value is used to identify the environmental parameters that are most dominant in determining habitat suitability. Parameters with higher contribution values are considered to have a greater influence on the variability of HSI values.

This sensitivity analysis was conducted under three different climate conditions, namely normal conditions, negative IOD, and positive IOD, allowing an evaluation of how the contribution of environmental parameters to the habitat suitability model varies under different climate variability scenarios. The Python scripts used for the sensitivity analysis are provided in the supplementary materials.

3. Results and discussion

3.1. Coastal upwelling along southern Java

The spatial distribution of SST during the JJAS period for 2016 (negative IOD), 2018 (normal conditions), and 2019 (positive IOD) along the southern coast of Java is shown in Figure 2. The results indicate that the IOD phenomenon strongly influences the spatial extent and intensity of coastal upwelling along southern Java. Upwelling is characterized by the presence of low SST values, reflecting the upward movement of cooler subsurface waters to the surface (Koropitan et al., 2021; Rachman et al., 2024). Under normal conditions in 2018, upwelling began to develop along the southern coast of Java in July,

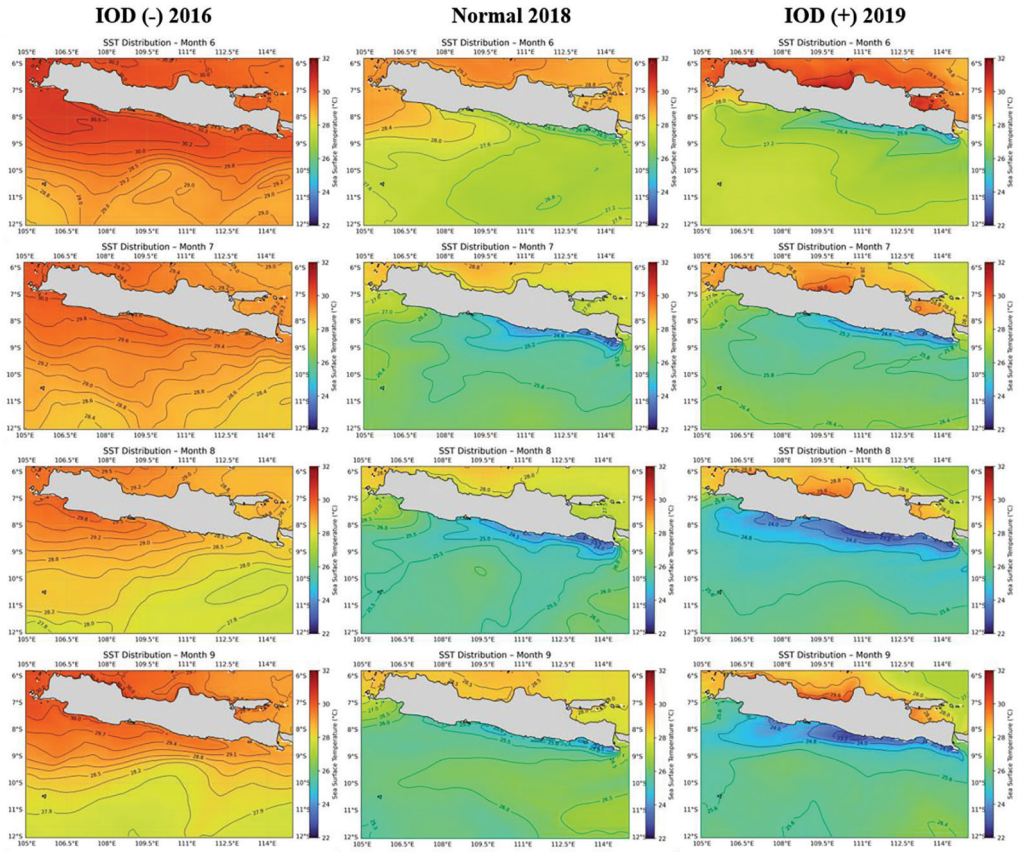

Figure 2

Spatial distribution of sea surface temperature (SST) along the southern coast of Java during June, July, August, and September under negative IOD conditions (2016), normal conditions (2018), and positive IOD conditions (2019).

as indicated by the emergence of SST values below 25°C (blue shading). The upwelling persisted until September, reaching its peak intensity in August 2018. During positive IOD conditions in 2019, upwelling was observed from JJAS, with a pronounced peak in August and a noticeably larger spatial extent compared to normal conditions in 2018. In contrast, during negative IOD conditions in 2016, upwelling was not detected throughout the JJAS period. Instead, SST values were significantly higher than those observed during the normal conditions in 2018. These findings are consistent with previous studies, which reported that positive IOD events enhance upwelling intensity, whereas negative IOD events suppress upwelling along the southern coast of Java (Rachman et al., 2024).

3.2. Habitat suitability model for *E. cottonii* aquaculture

The results of the habitat suitability model for *E. cottonii* aquaculture are presented in Figure 3. The model produces HSI values ranging from 0 to 1, where higher values indicate more suitable environmental conditions for *E. cottonii* cultivation. The results demonstrate that the occurrence of coastal upwelling exerts a negative influence on the habitat suitability model for *E. cottonii* aquaculture. Under normal conditions in 2018, the development of upwelling during July to September resulted in a decrease in HSI values, from a dominant value of 0.4 in June–0.2 in July and approximately 0.3 in August and September. Although upwelling is known to enhance primary productivity in coastal waters (Rachman et al., 2024), this increase was not accompanied by an improvement in HSI values for *E. cottonii* aquaculture.

A similar pattern was observed during positive IOD conditions in 2019, when increased upwelling intensity did not lead to improved habitat suitability. During this year, HSI values were predominantly 0.4 in June and declined to approximately 0.3 from July to September. In contrast, during negative IOD conditions in 2016, when upwelling was absent in the coastal waters of Cilacap and Kebumen, the habitat suitability model for *E. cottonii* aquaculture remained stable, with HSI

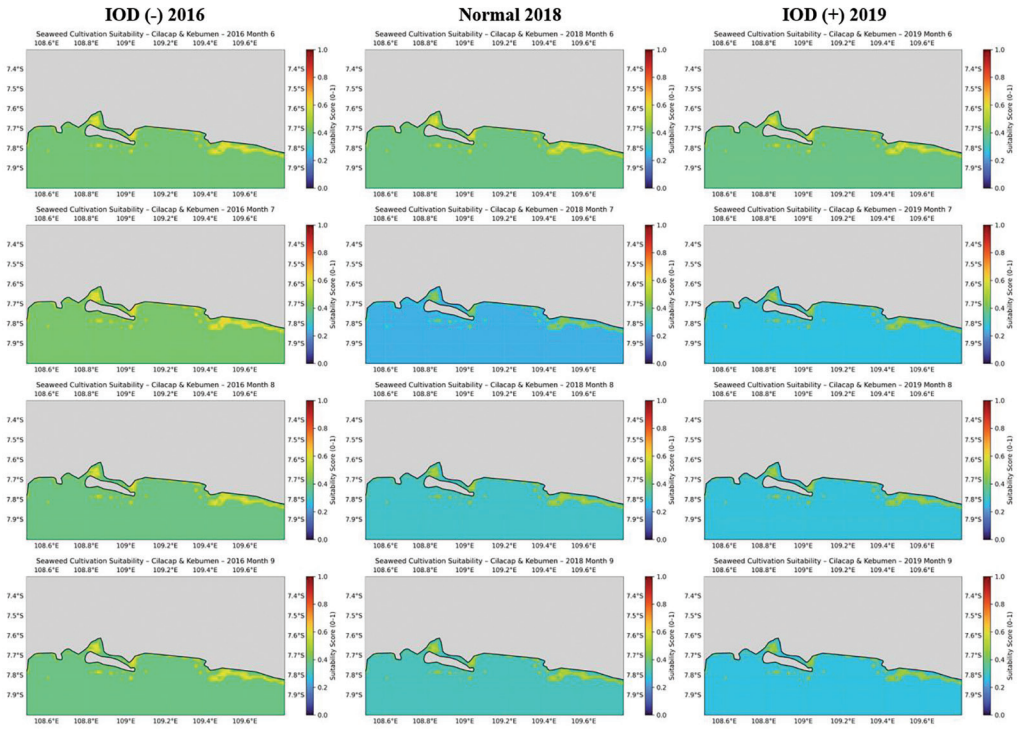

Figure 3

Habitat suitability model for *Eucheuma cottonii* aquaculture in the coastal waters of Cilacap and Kebumen under negative IOD (2016), normal (2018), and positive IOD (2019) conditions during June, July, August, and September.

values predominantly around 0.4 throughout the JJAS period (Figure 3). Based on Figure 3, the most suitable areas for *E. cottonii* cultivation, characterized by the highest HSI values across all months, are located in the coastal waters of Cilacap, particularly in the Segara Anakan region and along Teluk Penyu Beach (108.8°E–109.05°E). Additional suitable areas are identified in the eastern part of Kebumen waters, specifically from Suwuk Beach to Laguna Lembupuro Beach, within the longitude range of 109.42°E–109.8°E.

The HSI values obtained in this study ranged from 0 to 0.4 during the observation period. It should be emphasized that the model applied in this study follows a Boolean threshold approach based on five environmental parameters. Consequently, the HSI value represents the proportion of parameters that simultaneously meet the defined ecological suitability thresholds. Under this formulation, an HSI value of 0.4 indicates that two out of the five environmental parameters fall within their optimal ranges at a given grid cell. Within the framework of the classical Habitat Suitability Index developed under the Habitat Evaluation Procedures, the maximum value (HSI = 1) is only achieved when all environmental variables simultaneously reach their optimal conditions. Therefore, the absence of values ≥0.6 in this study indicates that no location satisfied at least three optimal environmental parameters simultaneously during the JJAS period (Zhang et al., 2025).

Habitat suitability classification in this study does not adopt universal thresholds (e.g., ≥0.6 as 'high suitability'), because habitat modeling literature highlights that classification boundaries are context-dependent and strongly influenced by model structure and analytical objectives (Kroth et al., 2025). Given the binary threshold approach and the regional-scale environmental datasets used in this study, HSI values are interpreted relatively, focusing on spatial and temporal differences among climate conditions rather than defining absolute suitability categories (Suresh et al., 2025). Accordingly, an HSI value of 0.4 should be interpreted as a relatively moderate level of suitability within the comparative framework of this study, rather than as an indication that the habitat is biologically optimal.

3.3. Environmental parameters

The upwelling process, which transports subsurface waters to the surface, not only alters SST but also modifies surface salinity, current velocity, and nutrient concentrations (Awo et al., 2022; Budiman et al., 2022;

Li et al., 2024). The SST range used to construct the habitat suitability model for *E. cottonii* aquaculture was 26°C–33°C (Manurung et al., 2021). Under normal conditions in 2018, SST in the coastal waters of Cilacap and Kebumen ranged from 27.3°C to 27.7°C in June, followed by a decrease in July to 24.9°C–25.4°C, 24.4°C–25.1°C in August, and 24.9°C–25.7°C in September (Figure 4). This decline in SST was associated with the occurrence of upwelling, resulting in SST values falling below the suitable range for *E. cottonii* cultivation during the upwelling period. During positive IOD conditions in 2019, enhanced upwelling intensity further reduced SST values, causing SST to deviate more strongly from the suitable range during July to September. SST values ranged from 25.9°C to 26.6°C in June, 24.7°C–25.3°C in July, 23.7°C–24.3°C in August, and 23.7°C–24.8°C in September. These results are consistent with Iskandar et al. (2022), who reported a significant SST decrease along the southern coast of Java due to upwelling processes during June–October 2019.

In contrast, negative IOD conditions in 2016 were characterized by significantly higher SST values compared to normal conditions, with SST ranging from 29.8°C to 30.3°C in June, 29.4°C–29.8°C in July, 29.2°C–29.6°C in August, and 29.6°C–29.8°C in September. These conditions resulted in SST values that remained within the suitable range for *E. cottonii* cultivation throughout the JJAS period. Koropitan et al. (2021) reported that during July–September 2016, monthly SST exceeded 29°C across parts of the western Sumatra coast and the southern coast of Java. This SST increase is attributed to negative IOD conditions, which extended their influence into the Java Sea and the southern Java upwelling system.

The salinity range used in the habitat suitability model for *E. cottonii* aquaculture was 25–35 PSU (Manurung et al., 2021). The salinity distribution during the JJAS period under negative IOD conditions (2016), normal conditions (2018), and positive IOD conditions (2019) remained entirely within the suitable range for seaweed cultivation. Under normal conditions in 2018, salinity values during JJAS ranged from 34.1 to 34.3 PSU, 34.5–34.6 PSU, 34.7–34.8 PSU, and 34.6–34.8 PSU, respectively. During negative IOD conditions in 2016, salinity values ranged from 33.2 to 33.4 PSU, 33.5–33.7 PSU, 33.7–33.8 PSU, and 33.3–34.5 PSU. During positive IOD conditions in 2019, salinity values ranged from 34.2 to 34.6 PSU, 34.6–34.7 PSU, 34.7–34.8 PSU, and 34.6–34.7 PSU (Figure 5).

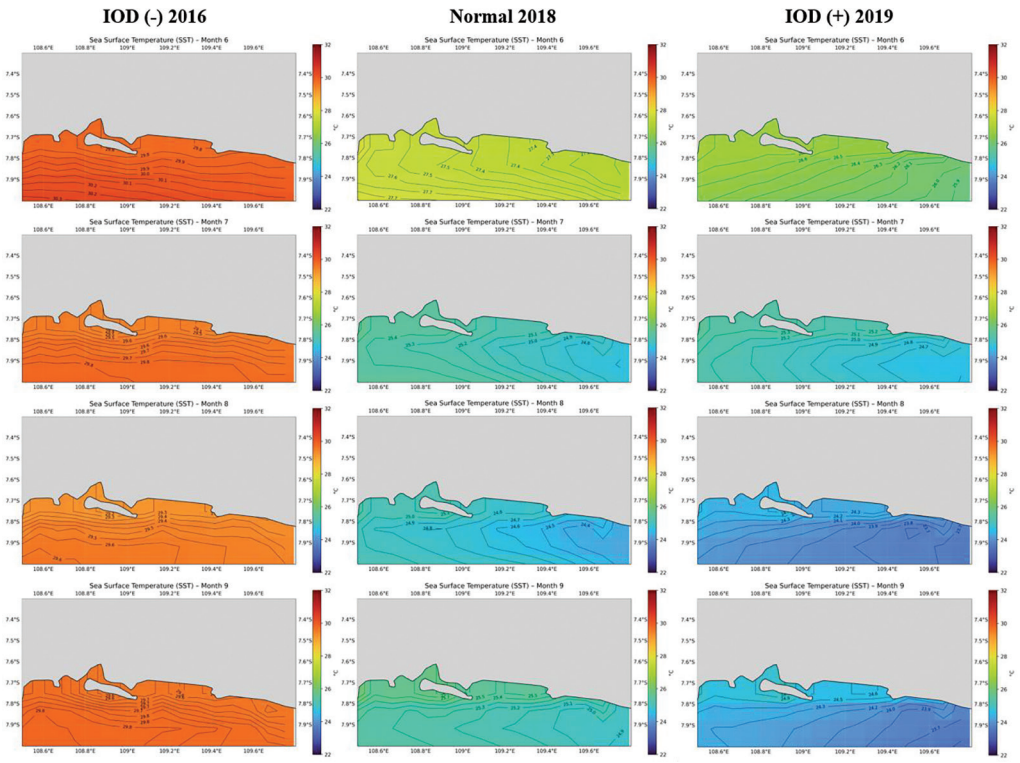

Figure 4

Spatial distribution of sea surface temperature (SST) in the coastal waters of Cilacap and Kebumen under negative IOD (2016), normal (2018), and positive IOD (2019) conditions during June, July, August, and September.

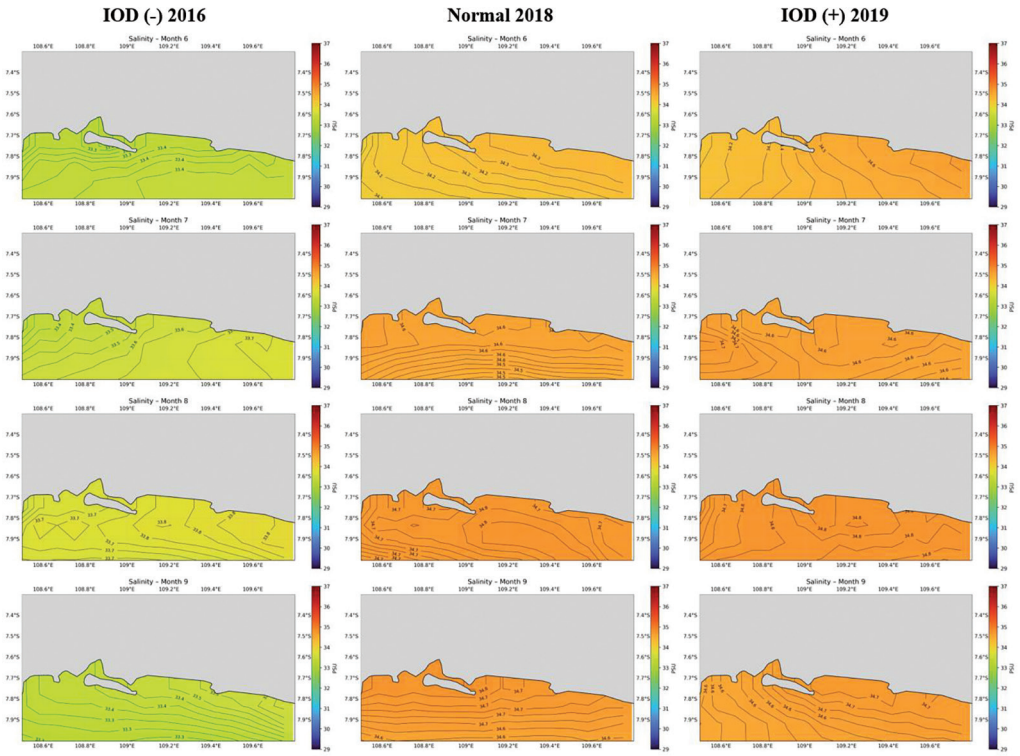

Figure 5

Spatial distribution of surface salinity in the coastal waters of Cilacap and Kebumen under negative IOD (2016), normal (2018), and positive IOD (2019) conditions during June, July, August, and September.

The increase in salinity associated with upwelling was relatively small, at approximately 0.2 PSU, while the occurrence of positive IOD conditions resulted in an additional increase of only about 0.1 PSU compared to normal conditions. In contrast, negative IOD conditions were associated with a decrease in surface salinity of up to 1 PSU. Huang et al. (2025) reported that during positive IOD events, equatorial easterly winds induce upwelling, strengthening anticyclonic salt advection, and leading to positive salinity anomalies. Chen et al. (2022) reported that during negative IOD events, surface salinity in the Indian Ocean can decrease by up to 2 PSU due to enhanced convergence, which increases freshwater transport.

Although salinity did not exhibit sufficient variation to fall outside the optimal range (25–35 PSU) throughout the entire observation period, equal weighting was retained in this model based on conceptual and methodological considerations. The HSI model employed was designed to represent suitability conditions simultaneously rather than to measure the relative sensitivity of each parameter to specific temporal variations. Thus, the stability of salinity within the optimal range does not imply that this variable is ecologically unimportant; rather, it indicates that during the JJAS period in the study area, salinity does not constitute a primary limiting factor for the cultivation of *E. cottonii*. Physiologically, tropical seaweeds are known to possess a relatively narrow salinity tolerance, and even minor changes can affect osmoregulatory processes and growth (Aris et al., 2021; Tilaar et al., 2025). Therefore, although interannual variation ranged only from 0.1 to 1 PSU (Figure 6), this parameter was retained to ensure that the model remains sensitive to potential extreme conditions beyond the analyzed period. Furthermore, habitat modeling literature emphasizes that assigning differential weights without a robust local quantitative basis may introduce subjective bias (Arsenault et al., 2025).

The nitrate concentration range used in the habitat suitability model for *E. cottonii* aquaculture was 0.1–4.4 mg L^{-1}, equivalent to 1.61–70.96 mmol m^{-3}. Under normal conditions in 2018, nitrate concentrations in the coastal waters of Cilacap and Kebumen were relatively low in June, at approximately 0.4 mmol m^{-3}. The onset of upwelling during July, August, and September increased nitrate concentrations to approximately 4.0, 4.6–5.0, and 3.8 mmol m^{-3}, respectively (Figure 7). Rachman et al. (2024) reported that upwelling processes transport

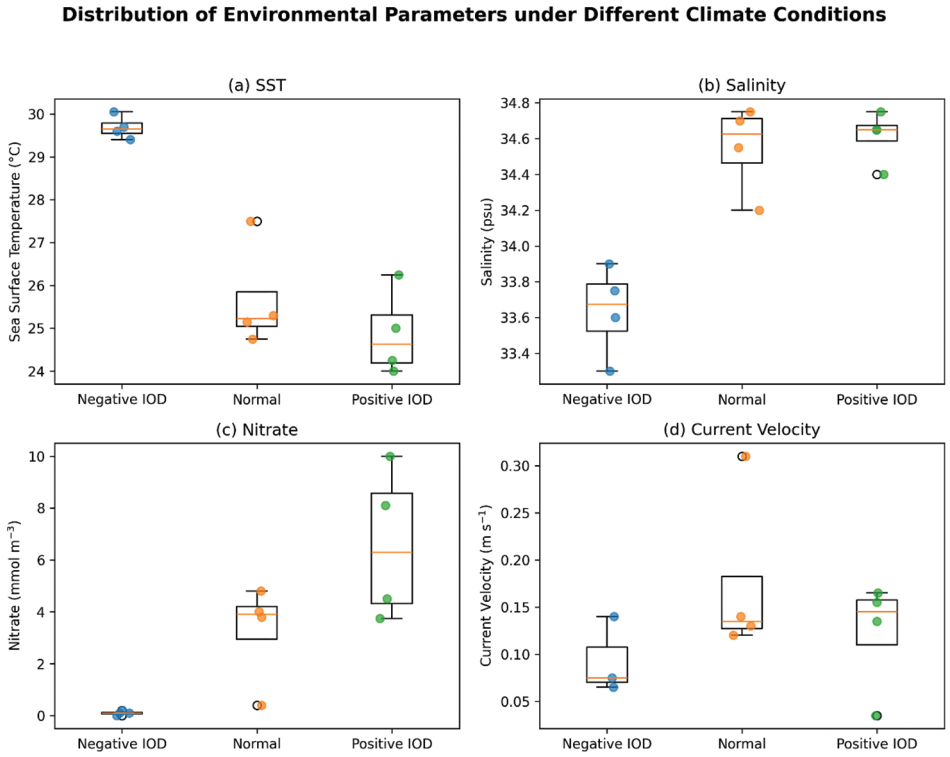

Figure 6

Boxplot distribution of environmental parameter under different climate conditions.

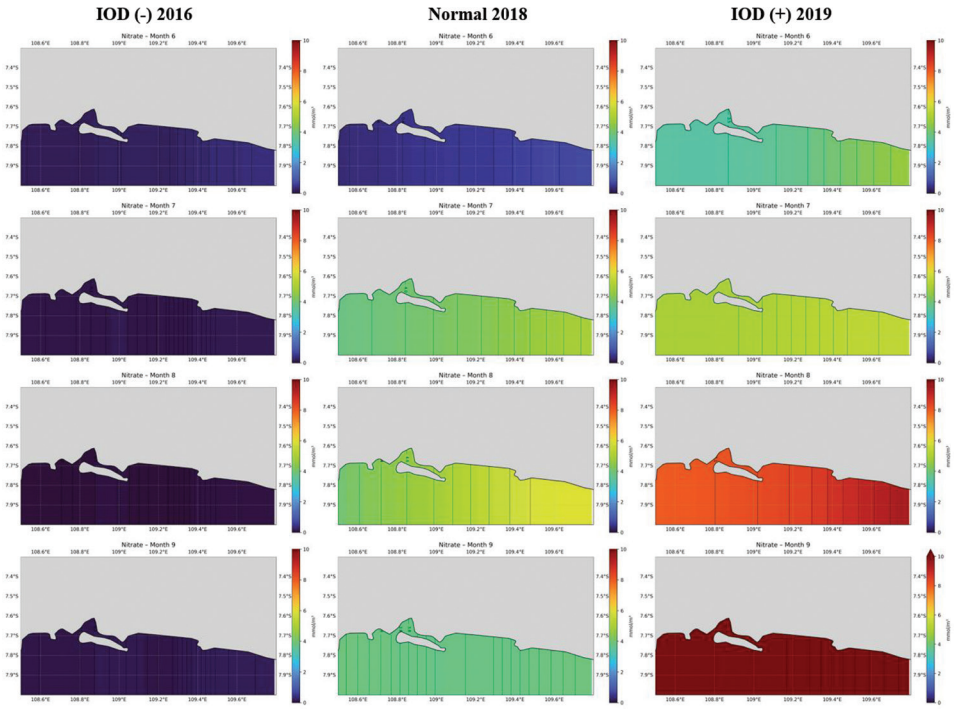

Figure 7

Spatial distribution of nitrate concentrations in the coastal waters of Cilacap and Kebumen under negative IOD (2016), normal (2018), and positive IOD (2019) conditions during June, July, August, and September.

nutrient-rich subsurface waters to the surface, thereby enhancing primary productivity in coastal waters.

During positive IOD conditions in 2019, nitrate concentrations increased markedly, reaching 3.5–4.0 mmol m^{-3} in June, approximately 4.5 mmol m^{-3} in July, 8.1 mmol m^{-3} in August, and exceeding 10 mmol m^{-3} in September. In contrast, during negative IOD conditions in 2016, nitrate concentrations decreased substantially, reaching approximately 0.2 mmol m^{-3} in June, 0.1 mmol m^{-3} in July, 0 mmol m^{-3} in August, and 0.1 mmol m^{-3} in September. Maysarah et al. (2022) demonstrated that positive IOD events are significantly associated with increased nitrate concentrations, particularly during the June to December period in southern Java waters, whereas the opposite pattern occurs during negative IOD events.

In the habitat suitability model applied in this study, a threshold-based Boolean approach was used, whereby any environmental parameter falling outside the defined optimal range, either below the lower limit or exceeding the upper limit, was automatically assigned a score of 0 (unsuitable). Therefore, during positive IOD conditions, when nitrate concentrations exceeded the upper threshold of the optimal range (Manurung et al., 2021), these values were classified as unsuitable for the nitrate parameter. Although nitrate enrichment associated with upwelling can enhance primary productivity, excessively high nutrient concentrations do not necessarily benefit the growth of cultivated macroalgae, as they may induce physiological imbalance and intensify competition with phytoplankton and epiphytic organisms (Hurd et al., 2014). Accordingly, in the context of *E. cottonii* cultivation, nitrate levels exceeding the optimal range were treated as suboptimal conditions within the habitat suitability assessment framework used in this study.

The current velocity range used in the habitat suitability model for *E. cottonii* aquaculture was 0.1–0.4 m s^{-1} (Manurung et al., 2021). Under normal conditions in 2018, current velocities in the coastal waters of Cilacap and Kebumen ranged from 0.04 to 0.20 m s^{-1} in June, 0.07–0.21 m s^{-1} in July, 0.03–0.23 m s^{-1} in August, and 0.26–0.36 m s^{-1} in September. The occurrence of IOD events, whether positive or negative, did not substantially alter current velocities in the coastal waters of Cilacap and Kebumen. During positive IOD conditions in 2019, current velocities ranged from 0.02 to 0.05 m s^{-1} in June, 0.12–0.15 m s^{-1} in July, 0.12–0.21 m s^{-1} in August, and 0.13–0.18 m s^{-1} in September. Similarly, during negative IOD conditions in 2016, current velocities ranged from 0.03 to 0.12 m s^{-1} in June and July, 0.10–0.18 m s^{-1} in August, and 0.03–0.10 m s^{-1} in September (Figure 8).

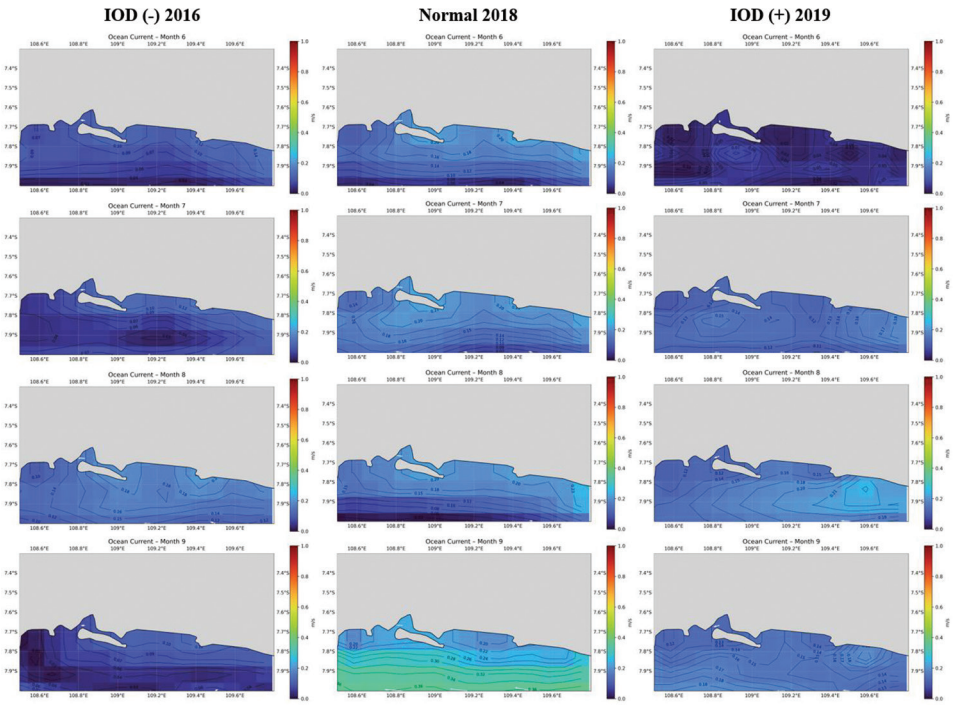

Figure 8

Spatial distribution of surface current velocity in the coastal waters of Cilacap and Kebumen under negative IOD (2016), normal (2018), and positive IOD (2019) conditions during June, July, August, and September.

These results differ from previous studies. Wijaya et al. (2024) reported that the south Java current (SJC) exhibits a negative relationship with IOD and ENSO during the June–August period, while Maysarah et al. (2022) found that the SJC strengthens during negative IOD events and weakens during positive IOD events. The discrepancy between the present results and previous findings is likely attributable to the relatively small spatial extent of the study area and its proximity to the coastline (≤8°S). Under these conditions, the influence of the SJC and large-scale climate variability on observed current velocities may be diminished, resulting in weaker detectable signals in the reanalysis data.

The bathymetry (water depth) range used in the habitat suitability model for *E. cottonii* aquaculture was 0.3–10 m (Manurung et al., 2021). As shown in Figure 9, suitable depth conditions were primarily confined to the eastern part of Kebumen waters, particularly within the longitude range of 109.35°E–109.8°E. Limited suitable areas were also identified in the coastal waters of Cilacap, specifically around the Segara Anakan region and Teluk Penyu Beach (Figure 9). These areas represent shallow coastal zones that meet the depth requirements for *E. cottonii* cultivation and largely determine the spatial distribution of high habitat suitability values observed in the habitat suitability model.

Among all environmental parameters used to construct the habitat suitability model, the spatial and temporal variation of SST (Figure 4) exhibits the strongest similarity to the spatial distribution and temporal variation of the HSI (Figure 3). This finding indicates that SST plays a dominant role in controlling the dynamics of habitat suitability for *E. cottonii* aquaculture.

The occurrence of upwelling, which lowers SST in the coastal waters of Cilacap and Kebumen, was found to negatively affect the habitat suitability of *E. cottonii* (Figure 3). This response contrasts with that of many other marine resources, whose productivity typically increases during upwelling events. These results raise an important question regarding the optimal timing of *E. cottonii* cultivation based on habitat suitability conditions, which should be addressed in future studies to support more effective cultivation recommendations.

Positive IOD events, which are associated with SST cooling in the coastal waters of Cilacap and Kebumen, did not exert a significant influence on the habitat suitability of *E. cottonii*. In contrast, negative IOD events, characterized by SST warming, had a significant positive effect on habitat suitability compared to normal conditions. This result highlights the critical sensitivity of *E. cottonii* cultivation to thermal conditions and suggests that warmer SSTs associated with negative IOD events provide more favorable environmental conditions for seaweed aquaculture in the study area. These results are consistent with previous findings by Lestari et al. (2019), who reported that during La Niña conditions characterized by relatively warmer SST and weaker upwelling, the potential area suitable for seaweed cultivation tends to be larger than during El Niño periods, which are typically associated with intensified upwelling.

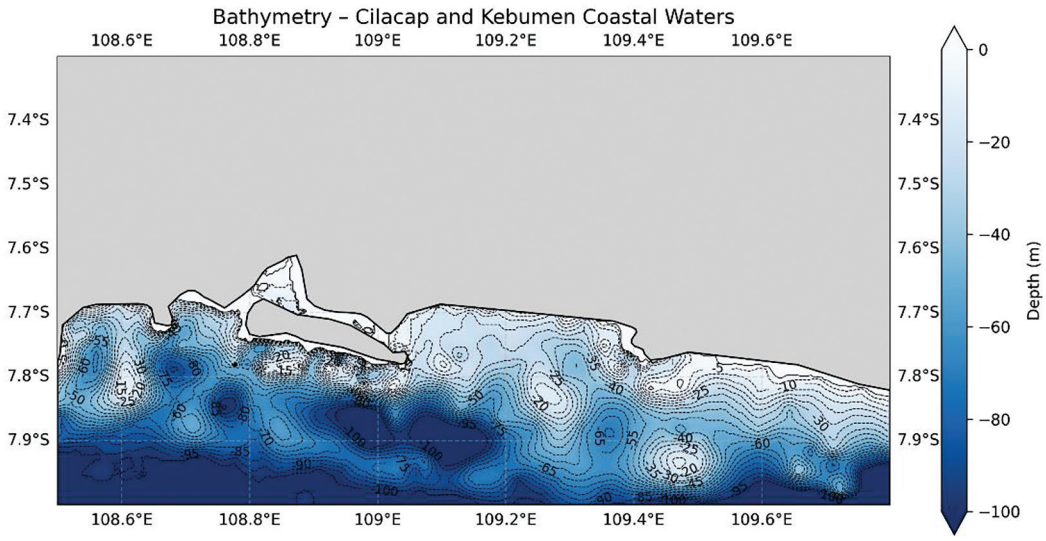

Figure 9

Bathymetric distribution in the coastal waters of Cilacap and Kebumen.

3.4. Kruskal–Wallis test analysis

Monthly midpoint values were used to represent environmental conditions and were treated as independent observations in the Kruskal–Wallis test to compare differences among climate conditions (negative IOD, normal, and positive IOD). The ranges and midpoint values of monthly environmental parameters under different climate conditions in the coastal waters of Cilacap and Kebumen are presented in Table 1, while the distribution of each parameter is illustrated using boxplots in Figure 6. The distribution of environmental parameters shows distinct responses to climate conditions. SST exhibits a clear decrease during positive IOD conditions, while nitrate concentration increases substantially, reflecting the intensification of coastal upwelling processes. In contrast, salinity and surface current velocity show relatively small variations among climate conditions, suggesting that these parameters are more strongly influenced by local factors than by regional climate variability. Because the environmental parameter data were not assumed to follow a normal distribution, a non-parametric approach using the Kruskal–Wallis test was considered the most appropriate method for evaluating differences among climate conditions.

The Kruskal–Wallis test results indicate significant differences in SST (p = 0.018 <0.05), salinity (p = 0.024 <0.05), and nitrate concentration (p = 0.018 <0.05) among climate conditions. In contrast, surface current velocity does not show a significant difference (p = 0.524 >0.05) (Table 2). In the Kruskal–Wallis test, the H statistic represents the magnitude of distributional differences among groups in this case, climate conditions (negative IOD, normal, and positive IOD) (Wilcox, 2012). Larger H values accompanied by significant p-values indicate a stronger influence of the differentiating factor, namely climate conditions (Rustin & Arifin, 2026; Saensouk et al., 2025). In this study, the H values obtained from the Kruskal–Wallis test are as follows: SST (H = 8.00), salinity (H = 7.45), nitrate concentration (H = 8.03), and surface current velocity (H = 1.29) (Table 2). The significant differences in SST, salinity, and nitrate concentration among climate conditions reflect the strong influence of basin-scale climate variability, particularly the IOD, on the oceanographic dynamics of the Cilacap and Kebumen coastal waters. During positive IOD conditions, the significant cooling of SST indicates an intensification of coastal upwelling along the southern coast of Java. This process promotes the upward transport of colder, more saline, and nutrient-rich subsurface water toward the surface, which directly explains the observed increase in nitrate concentrations during this period. Conversely, the opposite tendency occurs during negative IOD conditions (Awo et al., 2022; Budiman et al., 2022; Li et al., 2024). The absence of significant differences in surface current velocity among climate conditions suggests that surface current variability in this region is primarily controlled by local and regional factors, such as coastal topography, cross-shore circulation patterns, and intraseasonal wind fluctuations, rather than by interannual climate signals (Gu & Mao, 2024). This indicates that coastal environmental responses to climate variability are selective, with thermal and chemical parameters exhibiting higher sensitivity than dynamic parameters (Insan et al., 2025).

Overall, these results demonstrate that climate variability not only modulates the physical conditions of the ocean surface but also indirectly controls nutrient availability through coastal oceanographic processes. This pattern has important ecological implications, particularly for determining marine productivity and habitat suitability for fisheries and aquaculture activities in the southern coastal waters of Java.

3.5. Habitat model sensitivity analysis

The HSI sensitivity maps illustrate how spatial variations in HSI values occur when one environmental parameter is removed from the model under different climate conditions influenced by the IOD. In general, brighter colors on the maps indicate larger differences in HSI values, meaning that the removed parameter has a stronger influence on habitat suitability. Under Negative IOD conditions, noticeable changes in HSI occur when the nitrate and bathymetry (water depth) parameters are removed, particularly in offshore waters farther from the coastline. In contrast, removing current velocity results in relatively small and spatially homogeneous changes, indicating that current velocity has a relatively minor influence on habitat suitability in the waters of Cilacap and Kebumen during this phase (Figure 10).

Under Neutral IOD conditions, the sensitivity pattern appears more evenly distributed across the study area. Significant changes in HSI occur when salinity or sea surface salinity (SSS) and bathymetry are excluded from the model, indicating that these parameters play an important role in determining habitat suitability when oceanographic conditions are relatively stable. Meanwhile, during Positive IOD conditions, larger HSI differences appear when salinity and current velocity are removed, particularly in the southern offshore waters. This suggests that water mass dynamics, such as variations in salinity and current transport, become more influential factors during the positive IOD phase.

Table 1

Range and midpoint values of monthly environmental parameters under different climate conditions in the coastal waters of Cilacap and Kebumen.

Year/Condition	Month	Value range	Mean value
SST (°C)			
Negative IOD (2016)	June	29.8–30.3	30.05
	July	29.4–29.8	29.60
	August	29.2–29.6	29.40
	September	29.6–29.8	29.70
Normal (2018)	June	27.3–27.7	27.50
	July	24.9–25.4	25.15
	August	24.4–25.1	24.75
	September	24.9–25.7	25.30
Positive IOD (2019)	June	25.9–26.6	26.25
	July	24.7–25.3	25.00
	August	23.7–24.3	24.00
	September	23.7–24.8	24.25
Salinity (PSU)			
Negative IOD (2016)	June	33.2–33.4	33.30
	July	33.5–33.7	33.60
	August	33.7–33.8	33.75
	September	33.3–34.5	33.90
Normal (2018)	June	34.1–34.3	34.20
	July	34.5–34.6	34.55
	August	34.7–34.8	34.75
	September	34.6–34.8	34.70
Positive IOD (2019)	June	34.2–34.6	34.40
	July	34.6–34.7	34.65
	August	34.7–34.8	34.75
	September	34.6–34.7	34.65
Nitrate (mmol m^{-3})			
Negative IOD (2016)	June	0.2	0.20
	July	0.1	0.10
	August	0.0	0.00
	September	0.1	0.10
Normal (2018)	June	0.4	0.40
	July	4.0	4.00
	August	4.6–5.0	4.80
	September	3.8	3.80
Positive IOD (2019)	June	3.5–4.0	3.75
	July	4.5	4.50
	August	8.1	8.10
	September	>10	10
Current velocity (m s^{-1})			
Negative IOD (2016)	June	0.03–0.12	0.075
	July	0.03–0.12	0.075
	August	0.10–0.18	0.140
	September	0.03–0.10	0.065
Normal (2018)	June	0.04–0.20	0.120
	July	0.07–0.21	0.140
	August	0.03–0.23	0.130
	September	0.26–0.36	0.310
Positive IOD (2019)	June	0.02–0.05	0.035
	July	0.12–0.15	0.135
	August	0.12–0.21	0.165
	September	0.13–0.18	0.155

IOD, Indian Ocean Dipole; SST, sea surface temperature.

Table 2

Results of the Kruskal–Wallis test and their interpretation.

Parameter	*p*-value	*H*-value	Interpretation
SST	0.018	8.00	Significantly different
Salinity	0.024	7.45	Significantly different
Nitrate	0.018	8.03	Significantly different
Current velocity	0.524	1.29	Not significant

SST, sea surface temperature.

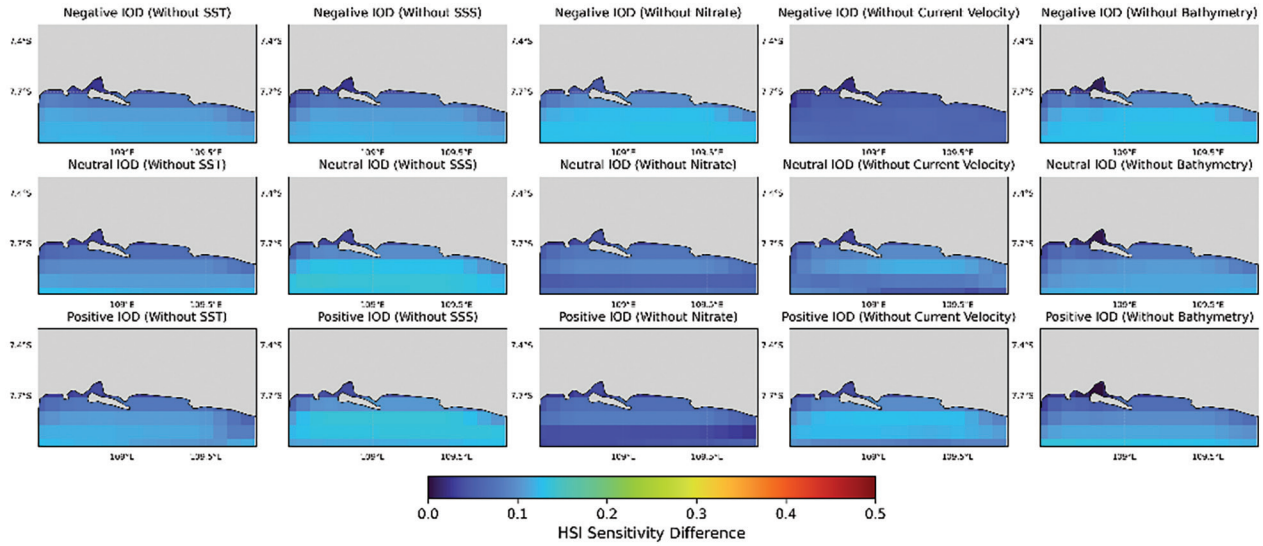

Figure 10

HSI Sensitivity Map.

The spatial patterns observed in the sensitivity maps are consistent with the parameter contribution analysis. The contribution values suggest that bathymetry (water depth) provides a relatively higher contribution compared to other parameters across the examined climate conditions, with contribution values ranging from 0.298 to 0.301, suggesting that water depth may represent an important baseline environmental factor influencing habitat suitability within the context of this HSI model. Salinity and SST also show relatively high contributions, ranging from 0.205 to 0.311 and 0.222–0.26, particularly under Neutral and Positive IOD conditions. In contrast, nitrate and current velocity exhibit relatively smaller contributions, ranging from 0.206 to 0.25 and 0.145–0.278, although they still play a role in shaping habitat suitability variability. Overall, the combination of sensitivity map analysis and parameter contribution values suggests that bathymetry (water depth) may play a relatively important role in shaping habitat suitability patterns, while other oceanographic parameters function as dynamic variables whose influence can vary depending on the prevailing IOD climate conditions (Figure 11). However, these results should be interpreted cautiously because the HSI model applied in this study is relatively simple and primarily exploratory. The contribution values represent relative influences within the model structure rather than definitive ecological causation.

4. Conclusion

The upwelling phenomenon in the southern Java waters tends to reduce the HSI for the cultivation of *E. cottonii*, particularly during July–September when upwelling intensity increases. Under normal conditions in 2018 and during the positive phase of the IOD in 2019, the strengthening of upwelling was associated with a decline in HSI values compared with June. In contrast, during the negative IOD phase in 2016, when upwelling signals were relatively weak, HSI

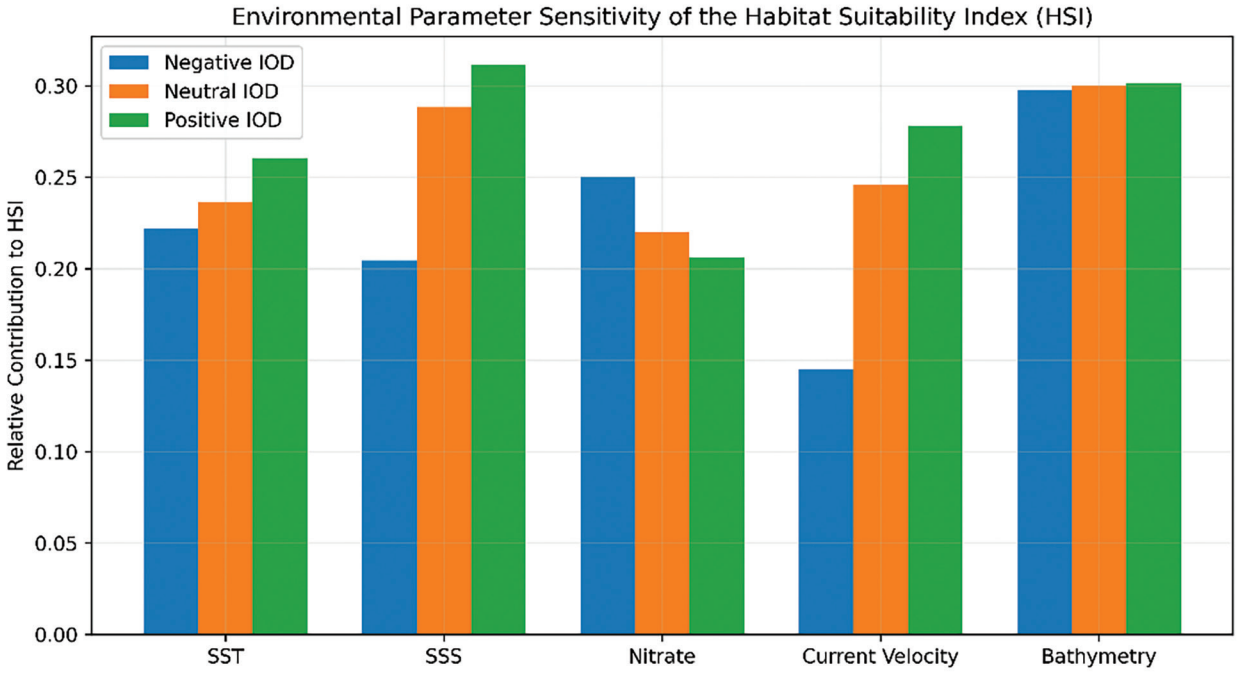

Figure 11

Environmental Parameter Sensitivity of HSI.

values remained comparatively stable throughout the July–September period, with dominant values around 0.4. However, this interpretation should be considered with caution because the analysis of negative IOD conditions in this study is based on only a single year of observation, which is insufficient for drawing long-term climatic generalizations. The results of the Kruskal–Wallis test indicate that SST, salinity, and nitrate concentration exhibit significant differences among climate conditions, whereas surface current velocity does not show a significant difference. The combination of sensitivity map analysis and parameter contribution values indicates suggests that bathymetry (water depth) may play a relatively important role in shaping habitat suitability patterns, while other oceanographic parameters (SST, salinity, nitrate, and surface current velocity) function as dynamic variables whose influence can vary depending on the prevailing IOD climate conditions. Nevertheless, the relationship between IOD phases and habitat suitability identified in this study should be interpreted as a preliminary and exploratory indication rather than a generalized climatic pattern. Future studies incorporating longer time series and a greater number of IOD events are necessary to statistically evaluate the consistency of this pattern and to improve the robustness of climate–habitat relationships at broader climatic scales.

Acknowledgments

The authors would like to thank the Copernicus Marine Service for providing the oceanographic reanalysis datasets and the General Bathymetric Chart of the Oceans (GEBCO) for supplying bathymetric data used in this study. We also acknowledge the Bureau of Meteorology (BOM) for providing the IOD index data. The authors are sincerely grateful to the anonymous reviewers and editor for their insightful comments and constructive suggestions, which helped improve the scientific rigor, clarity, and overall quality of this manuscript.

References

Arbit, N. I. S., Lestari, D., Erwin, E., Syamsudin, F., Mannan, A., & Thabrani, M. (2024). Suitability water quality parameters for *Eucheuma cottonii* culture at Majene Waters. *DEPIK Учредители: Institute of Postgraduate Studies, Syiah Kuala University, 13*(2), 192-200. https://doi.org/10.13170/depik.13.2.35688

Aris, M., Muchdar, F., & Labenua, R. (2021). Study of seaweed *Kappaphycus alvarezii* explants growth in the different salinity concentrations. *Jurnal Ilmiah Perikanan Dan Kelautan, 13*(1), 97-105. https://doi.org/10.20473/jipk.v13i1.19842

Arsenault, S., Linner, R., & Chen, Y. (2025). Evaluating effects of data quality and variable weighting on habitat suitability modelling. *Ecological Informatics, 87*, Article 103086. https://doi.org/10.1016/j.ecoinf.2025.103086

Awo, F. M., Rouault, M., Ostrowski, M., Tomety, F. S., Da-Allada, C. Y., & Jouanno, J. (2022). Seasonal cycle of sea surface salinity in the Angola upwelling system. *Journal of Geophysical Research: Oceans, 127*(7), Article e2022JC018518. https://doi.org/10.1029/2022JC018518

Bertelli, C. M., Stokes, H. J., Bull, J. C., & Unsworth, R. K. F. (2022). The use of habitat suitability modelling for seagrass: A review. *Frontiers in Marine Science, 9*, Article 997831. https://doi.org/10.3389/fmars.2022.997831

Budiman, A. S., Bengen, D. G., Nurjaya, I. W., Arifin, Z., & Ismail, M. F. A. (2022). A comparison of the three upwelling indices in the South Java sea shelf. *Chiang Mai University Journal of Natural Sciences, 21*(3), Article e2022044. https://doi.org/10.12982/CMUJNS.2022.044

Casadebaig, P., Gauffreteau, A., Landré, A., Langlade, N. B., Mestries, E., Sarron, J., Trépos, R., Vincourt, P., & Debaeke, P. (2022). Optimized cultivar deployment improves the efficiency and stability of sunflower crop production at national scale. *Theoretical and Applied Genetics, 135*(11), 4049–4063. https://doi.org/10.1101/2020.09.21.306076

Chen, S., Cha, J., Qiu, F., Jing, C., Qiu, Y., & Xu, J. (2022). Sea surface salinity anomaly in the bay of Bengal during the 2010 extremely negative IOD event. *Remote Sensing, 14*(24), Article 6242. https://doi.org/10.3390/rs14246242

Damis, D., & Saenong, M. (2020). Analisis kualitas air dalam penentuan lokasi budidaya rumput laut (*Eucheuma cottonii*) di kawasan Teluk Parepare. *Journal of Indonesian Tropical Fisheries, 3*(2), 205–213. https://doi.org/10.33096/joint-fish.v3i2.79

Gokturk, E. N., Bartlett, B. S., Erisman, B., Heyman, W., & Asch, R. G. (2022). Loss of suitable ocean habitat and phenological shifts among grouper and snapper spawning aggregations in the Greater Caribbean under climate change. *Marine Ecology Progress Series, 699*, 91–115. https://doi.org/10.3354/meps14165

Gu, H., & Mao, Y. (2024). Multi-timescale characteristics of southwestern Australia nearshore surface current and its response to ENSO revealed by high-frequency radar. *Remote Sensing, 16*(1), Article 209. https://doi.org/10.3390/rs16010209

Hafiz, M., Widagdo, S., & Prasita, V. D. (2024). Eksistensi upwelling Pada Fase Netral di Perairan Selatan Jawa. *J-Tropimar, 6*(1), 1–10. https://doi.org/10.30649/jrkt.v6i1.77

Horii, T., Ueki, I., Siswanto, E., & Iskandar, I. (2023). Long-term shift and recent early onset of chlorophyll-a bloom and coastal upwelling along the southern coast of Java. *Frontiers in Climate, 5*, Article 1050790. https://doi.org/10.3389/fclim.2023.1050790

Huang, K., Wang, D., Zu, T., & Vithana, M. (2025). IOD-driven seesaw mode of upper-ocean salinity variability in the central and eastern tropical Indian Ocean. *Environmental Research Letters, 20*(10), Article 104045. https://doi.org/10.1088/1748-9326/ae0056

Hurd, C. L., Harrison, P. J., Bischof, K., & Lobban, C. S. (2014). *Seaweed ecology and physiology*. Cambridge University Press. https://doi.org/10.1017/CBO9781139192637.007

Insan, K., Patty, W., Manembu, I. S., Djamaluddin, R., Kusen, D. J., Paulus, J. J. H., Sumilat, D. A., & Rogi, J. E. X. (2025). Variability of oceanographic parameters during and after tropical cyclone Kammuri in Talaud Islands waters. *Jurnal Pesisir Dan Laut Tropis, 13*(2), 188–200. https://doi.org/10.35800/jplt.13.2.2025.62642

Iskandar, I., Lestari, D. O., Saputra, A. D., Setiawan, R. Y., Wirasatriya, A., Susanto, R. D., Mardiansyah, W., Irfan, M., Rozirwan, R., & Setiawan, J. D. (2022). Extreme positive Indian Ocean Dipole in 2019 and its impact on Indonesia. *Sustainability, 14*(22), Article 15155. https://doi.org/10.3390/su142215155

Koropitan, A. F., Kholilullah, I., & Yusfiandayani, R. (2021). Modeling mackerel tuna (*Euthynnus affinis*) habitat in southern coast of Java: Influence of seasonal upwelling and negative IOD. *HAYATI Journal of Biosciences, 28*(4), 271–285. https://doi.org/10.4308/hjb.28.4.271-285

Kroth, F., Kuhwald, K., Schneider, T., & Oppelt, N. (2025). Habitat suitability and species distribution modelling in lake macrophyte research: A systematic review. *Ecological Indicators, 179*, Article 114141. https://doi.org/10.1016/j.ecolind.2025.114141

Lan, K.-W., Evans, K., & Lee, M.-A. (2013). Effects of climate variability on the distribution and fishing conditions of yellowfin tuna (*Thunnus albacares*) in the western Indian Ocean. *Climatic Change, 119*(1), 63–77. https://doi.org/10.1007/s10584-012-0637-8

Lan, K.-W., Lee, M.-A., Wang, S.-P., & Chen, Z.-Y. (2015). Environmental variations on swordfish (*Xiphias gladius*) catch rates in the Indian Ocean. *Fisheries Research, 166*, 67–79. https://doi.org/10.1016/j.fishres.2014.08.010

Lase, P. J. R., Tuhumury, S. F., & Waas, H. J. D. (2020). Analisis Kesesuaian Lokasi Budidaya Rumput Laut (*Eucheuma cottonii*) dengan Menggunakan Sistem Informasi Geografis di Perairan Teluk Ambon Baguala. *TRITON: Jurnal Manajemen Sumberdaya Perairan, 16*(2), 77–83. https://doi.org/10.30598/TRITONvol16issue2page77-83

Lestari, D. A., Susiloningtyas, D., & Handayani, T. (2019). Potential Region for development of seaweed genus *Eucheuma cottonii* based on ENSO variability in east coast of Tarakan Island, Indonesia. *IOP Conference Series: Earth and Environmental Science, 284*(1), Article 12030. https://doi.org/10.1088/1755-1315/284/1/012030

Li, H., Guo, P., Liu, G., Suo, A., Zhou, W., Yue, W., Jiao, M., & Zhang, L. (2024). Numerical study of the upwelling and downwelling effects of artificial reefs along tidal cycles in the Pearl River Estuary. *Journal of Environmental Management, 365*, Article 121486. https://doi.org/10.1016/j.jenvman.2024.121486

Manurung, D. F., Rosmasita, R., Windarti, W., Ghazali, T. M., & Sibuea, N. U. S. (2021). Suitability of seaweed culture (*Eucheuma cottonii*) in the Sorkam Barat Sub-District, Tapanuli Tengah Indonesia. *IOP Conference Series: Earth and Environmental Science, 934*(1), Article 12012. https://doi.org/10.1088/1755-1315/934/1/012012

Maysarah, S., Sartimbul, A., & Pranowo, W. S. (2022). Analisis Variabilitas Nitrat dalam Hubungan dengan El Nino Southern Oscillation (ENSO) dan Indian Ocean Dipole (IOD) di Perairan Selat Bali dan Sekitarnya: Analysis of variability of nitrate in corellation with El Nino southern oscillation (ENSO) and Indian Ocean Dipole (IOD) in the Bali Strait and surroundings. *Jurnal Hidropilar, 8*(2), 91–100. https://doi.org/10.37875/hidropilar.v8i2.251

Napitupulu, G. (2025). Spatiotemporal variability of coastal upwelling in response to monsoonal forcing and semi-enclosed basins in the indonesian and adjacent seas. *Ocean Dynamics, 75*(7), 1–20. https://doi.org/10.1007/s10236-025-01706-2

Numberi, Y., Budi, S., & Salam, S. (2020). Analisis oseanografi dalam mendukung budidaya rumput laut (*Eucheuma cottonii*) di Teluk Sarawandori Distrik Kosiwo Yapen-Papua. *Urban and Regional Studies Journal, 2*(2), 71–75. https://doi.org/10.35965/ursj.v2i2.569

Oktaviani, D., Handoyo, G., Helmi, M., Kunarso, K., & Wirasatriya, A. (2021). Karakteristik upwelling pada Periode Indian Ocean Dipole (IOD) Positif di Perairan Selatan Jawa Barat. *Indonesian Journal of Oceanography, 3*(4), 354–361. https://doi.org/10.14710/ijoce.v3i4.12081

Rachman, H. A., Setiawati, M. D., Hidayah, Z., Syah, A. F., Nandika, M. R., Lumban-Gaol, J., As-syakur, A. R., & Syamsudin, F. (2024). Dynamic of upwelling variability in southern Indonesia region revealed from satellite data: Role of ENSO and IOD. *Journal of Sea Research, 202*, Article 102543. https://doi.org/10.1016/j.seares.2024.102543

Rochmatika, E., & Bahtiar, S. A. (2023). The effect of upwelling on water productivity based on chlorophyll-a parameters in Sumatra and Java Waters (Edge of Jakarta Bay, South Lampung and South Coast of Central Java). *Proceeding International Conference on Religion, Science and Education, 2*(2023), 945–949.

Rusdi, W. A. (2018). Analysis of suitability and carrying capacity of waters for seaweed (*Eucheuma cottonii*) cultivation business in Mandar Bay, West Sulawesi of Indonesia. *Russian Journal of Agricultural and Socio-Economic Sciences, 82*(10), 295–300. https://doi.org/10.18551/rjoas.2018-10.34

Rustin, S. N., & Arifin, S. (2026). A review of Kruskal-Wallis test applications in scientific research. *Journal of Actuarial, Finance and Risk Management, 4*(2), 36–46. http://dx.doi.org/10.33021/jafrm.v4i2.6301.g2413

Saensouk, P., Saensouk, S., Thuy, M. T. P., Taesuk, N., Ruannakarn, P., Phimpha, S., & Boonma, T. (2025). Diversity and its implications of curcuma Subgenus Hitcheniopsis (Zingiberaceae) with a new record for Vietnam. *Diversity, 17*(11), Article 778. https://doi.org/10.3390/d17110778

Salihin, A., Muhiddin, A. H., & Yasir, I. (2019). Evaluation study of *Eucheuma cottonii* species of seaweed cultivation based on oceanographic parameters in Pasiea, Bonegunu Subdistrict, North Buton District. *Jurnal Ilmu Kelautan SPERMONDE, 5*(2), 51–56. https://doi.org/10.20956/jiks.v5i2.8930

St Madina, M., Syafiuddin, S., Samawi, M. F., Muhiddin, A. H., & Hatta, M. (2022). Water quality of seaweed cultivation (*Eucheuma cottonii*) location in Old Takalar, Mappakasunggu District, Takalar Regency. *Jurnal Ilmu Kelautan SPERMONDE, 8*(2), 28–36. https://doi.org/10.20956/jiks.v8i2.19770

Stephenson, F., Rowden, A. A., Anderson, O. F., Pitcher, C. R., Pinkerton, M. H., Petersen, G., & Bowden, D. A. (2021). Presence-only habitat suitability models for vulnerable marine ecosystem indicator taxa in the South Pacific have reached their predictive limit. *ICES Journal of Marine Science, 78*(8), 2830–2843. https://doi.org/10.1093/icesjms/fsab162

Stuart, C. E., Wedding, L. M., Pittman, S. J., & Green, S. J. (2021). Habitat suitability modeling to inform seascape connectivity conservation and management. *Diversity, 13*(10), Article 465. https://doi.org/10.3390/d13100465

Sun, Y., Zhang, H., Jiang, K., Xiang, D., Shi, Y., Huang, S., Li, Y., & Han, H. (2024). Simulating the changes of the habitats suitability of chub mackerel (*Scomber japonicus*) in the high seas of the North Pacific Ocean using ensemble models under medium to long-term future climate scenarios. *Marine Pollution Bulletin, 207*, Article 116873. https://doi.org/10.1016/j.marpolbul.2024.116873

Suresh, N., Dubey, M., Hardas, M. S., Kumar, M. A., Narsingan, L. S., & Karpagavalli, S. (2025). Modeling species distribution and habitat suitability with machine learning approaches. *International Journal of Environmental Sciences, 11*(23s), 5353–5363. https://doi.org/10.64252/nbbcax54

Tilaar, S., Wullur, S., & Angkouw, E. D. (2025). The effect of salinity on the growth of *Kappaphycus alvarezii*. *Jurnal Ilmiah PLATAX, 13*(2), 335–340. https://doi.org/10.35800/jip.v13i2.58380

Ukhti, F., Manurug, Z. K., & Mahendra, M. D. (2021). Perbandingan Teknik boolean dengan weighted overlay Dalam Analisis Potensi Longsor di Banjarmasin. *Jurnal Geosains Dan Remote Sensing, 2*(1), 25–32. https://doi.org/10.23960/jgrs.2021.v2i1.53

Utama, R. Z., & Handayani, T. (2018). Suitability between ocenography and seaweed (*Eucheuma cottonii*) cultivation potential in Tidung Island with geographic information system (GIS). *E3S Web of Conferences, 73*, Article 12009. https://doi.org/10.1051/e3sconf/20187312009

Wabang, I. L., & Plaimo, P. E. (2024). Coastal resources study for the suitability of seaweed (*Eucheuma cottonii*) cultivation land in Pulau Lapang Waters, Pantar Barat District, Alor District. *Berkala Perikanan Terubuk, 52*(2), 2251–2256.

Wahyuni, S., Nursan, M., & Hidayati, A. (2023). Analysis of red algae seaweed (*Eucheuma cottonii*) cultivation in Jerowaru District, Lombok regency. *Jurnal Biologi Tropis, 23*(2), 450–455. https://doi.org/10.29303/jbt.v23i2.4878

Wang, G., Cai, W., Santoso, A., Abram, N., Ng, B., Yang, K., Geng, T., Doi, T., Du, Y., & Izumo, T. (2024). The Indian Ocean Dipole in a warming world. *Nature Reviews Earth & Environment, 5*(8), 588–604. https://doi.org/10.1038/s43017-024-00573-7

Wan, G.-Z., Li, Q.-Q., Jin, L., & Chen, J. (2024). Integrated approach to predicting habitat suitability and evaluating quality variations of *Notopterygium franchetii* under climate change. *Scientific Reports, 14*(1), Article 26927. https://doi.org/10.1038/s41598-024-77824-6

Wen, L., Zhang, H., Fang, Z., & Chen, X. (2025). The effects of climate change on *Sthenoteuthis oualaniensis* habitats in the Northern Indian Ocean. *Animals, 15*(4), Article 573. https://doi.org/10.3390/ani15040573

Widagdo, S., Prasita, V. D., & Hafiz, M. (2025). Upwelling intensity during Indian Ocean Dipole period in southern waters of Java. *IOP Conference Series: Earth and Environmental Science, 1473*(1), Article 12015. https://doi.org/10.1088/1755-1315/1473/1/012015

Wijayanto, D., Bambang, A. N., Nugroho, R. A., & Kurohman, F. (2020). The impact of planting distance on productivity and profit of *Eucheuma cottonii* seaweed cultivation in Karimunjawa Islands, Indonesia. *Aquaculture, Aquarium, Conservation & Legislation, 13*(4), 2170–2179.

Wijaya, Y. J., Wisha, U. J., Rejeki, H. A., & Ismunarti, D. H. (2024). Variability of the South Java current from 1993 to 2021, and its relationship to ENSO and IOD events. *Asia-Pacific Journal of Atmospheric Sciences, 60*(1), 65–79. https://doi.org/10.1007/s13143-023-00336-2

Wilcox, R. R. (2012). *Introduction to robust estimation and hypothesis testing*. Academic press. https://doi.org/10.1016/B978-0-12-804733-0.00007-X

Zhang, H., Zhao, C., Wang, J., Chen, X., & Lei, L. (2025). Designing of high-performance species habitat suitability index model. *Fisheries Research, 291*, Article 107548. https://doi.org/10.1016/j.fishres.2025.107548

Supplementary Material Kruskal–Wallis Test & Boxplot Syntax

In [1]:

```
import numpy as np
import pandas as pd
from scipy.stats import kruskal
```

In [2]:

```
# SST nilai tengah (JJAS)
sst_iod_neg = np.array([30.05, 29.60, 29.40, 29.70])    # 2016
sst_normal = np.array([27.50, 25.15, 24.75, 25.30])    # 2018
sst_iod_pos = np.array([26.25, 25.00, 24.00, 24.25])   # 2019
```

In [3]:

```
H_sst, p_sst = kruskal(sst_iod_neg, sst_normal, sst_iod_pos)
print("SST: H =", H_sst, "p-value =", p_sst)
```

SST: H = 8.0 p-value = 0.018315638888734186

In [4]:

```
sal_iod_neg = np.array([33.30, 33.60, 33.75, 33.90])
sal_normal = np.array([34.20, 34.55, 34.75, 34.70])
sal_iod_pos = np.array([34.40, 34.65, 34.75, 34.65])
```

In [5]:

```
H_sal, p_sal = kruskal(sal_iod_neg, sal_normal, sal_iod_pos)
print("Salinitas: H =", H_sal, "p-value =", p_sal)
```

Salinitas: H = 7.4463028169014125 p-value = 0.02415771692662978

In [6]:

```
nit_iod_neg = np.array([0.20, 0.10, 0.00, 0.10])
nit_normal = np.array([0.40, 4.00, 4.80, 3.80])
nit_iod_pos = np.array([3.75, 4.50, 8.10, 10.00])  # nilai konservatif
```

In [7]:

```
H_nit, p_nit = kruskal(nit_iod_neg, nit_normal, nit_iod_pos)
print("Nitrat: H =", H_nit, "p-value =", p_nit)
```

Nitrat: H = 8.028070175438597 p-value = 0.018060372821376538

In [8]:

```
cur_iod_neg = np.array([0.075, 0.140, 0.065])
cur_normal = np.array([0.120, 0.140, 0.130, 0.310])
cur_iod_pos = np.array([0.035, 0.135, 0.165, 0.155])
```

In [9]:

```
H_cur, p_cur = kruskal(cur_iod_neg, cur_normal, cur_iod_pos)
print("Arus: H =", H_cur, "p-value =", p_cur)
```

Arus: H = 1.291856925418572 p-value = 0.5241756385721527

In [17]:

```
import numpy as np
import matplotlib.pyplot as plt
import os

# =========================
# Output directory
# =========================
output_dir = r"D:\RL\tambahan"
os.makedirs(output_dir, exist_ok=True)

# =========================
# Midpoint data (JJAS)
# =========================

# Sea Surface Temperature (°C)
sst_neg = np.array([30.05, 29.60, 29.40, 29.70])
sst_norm = np.array([27.50, 25.15, 24.75, 25.30])
sst_pos = np.array([26.25, 25.00, 24.00, 24.25])


# Salinity (psu)
sal_neg = np.array([33.30, 33.60, 33.75, 33.90])
sal_norm = np.array([34.20, 34.55, 34.75, 34.70])
sal_pos = np.array([34.40, 34.65, 34.75, 34.65])
```

```
# Nitrate (mmol m-3)
nit_neg = np.array([0.20, 0.10, 0.00, 0.10])
nit_norm = np.array([0.40, 4.00, 4.80, 3.80])
nit_pos = np.array([3.75, 4.50, 8.10, 10.00])

# Current velocity (m s-1)
cur_neg = np.array([0.075, 0.140, 0.065])
cur_norm = np.array([0.120, 0.140, 0.130, 0.310])
cur_pos = np.array([0.035, 0.135, 0.165, 0.155])

# ============================
# Plot setup
# ============================
fig, axes = plt.subplots(2, 2, figsize=(10, 8))
labels = ['Negative IOD', 'Normal', 'Positive IOD']

def boxplot_with_points(ax, data, ylabel, title):
    ax.boxplot(data, labels=labels, showfliers=True)
    for i, y in enumerate(data, start=1):
```

```
        x = np.random.normal(i, 0.04, size=len(y)) ax.plot(x, y, 'o', alpha=0.7)
    ax.set_ylabel(ylabel) ax.set_title(title)


# ============================
# Subplots
# ============================
boxplot_with_points(
    axes[0, 0],
    [sst_neg, sst_norm, sst_pos], 'Sea
    Surface Temperature (°C)', '(a)
    SST'
)

boxplot_with_points(
    axes[0, 1],
    [sal_neg, sal_norm, sal_pos], 'Salinity
    (psu)',
    '(b) Salinity'
)

boxplot_with_points(
    axes[1, 0],
    [nit_neg, nit_norm, nit_pos], 'Nitrate
    (mmol m$^{-3}$)',
    '(c) Nitrate'
)
```

boxplot_with_points(

axes[1, 1],

[cur_neg, cur_norm, cur_pos],

'Current Velocity (m s^{-1})', '(d)

Current Velocity'

```
)

# ========================
# Final layout & save
# ========================
fig.suptitle(
    'Distribution of Environmental Parameters under Different Climate Conditions
    fontsize=14,
    fontweight='bold'
)

plt.tight_layout(rect=[0, 0, 1, 0.95])
plt.savefig(
    os.path.join(output_dir, 'Boxplot_Environmental_Parameters_KruskalWallis.png
    dpi=300
)
plt.close()
```

Supplementary Material Habitat Suitability Syntax

In [ ]:

```
#HABITAT SUITABILITY SYNTAX
import xarray as xr
import numpy as np
import matplotlib.pyplot as plt
import os
import cartopy.crs as ccrs
import cartopy.feature as cfeature
from scipy.ndimage import gaussian_filter

# === Load Dataset ===
ds_sst = xr.open_dataset("D:/RL/SST_jateng_2016.nc")
ds_sal = xr.open_dataset("D:/RL/Salinity_jateng_2016.nc")
ds_nit = xr.open_dataset("D:/RL/Nitrat_jateng_2016.nc")
ds_ars = xr.open_dataset("D:/RL/Arus_jateng_2016.nc")
ds_bati = xr.open_dataset("D:/RL/Bati.nc")

# === Take the main variable ===
sst = ds_sst['thetao']
sal = ds_sal['so']
nit = ds_nit['no3']
uo = ds_ars['uo']
vo = ds_ars['vo']
bati = ds_bati[list(ds_bati.data_vars)[0]]  # ambil variabel pertama

# === Take sea level if there is depth ===
for var_name in ['sst', 'sal', 'nit', 'uo', 'vo']:
    var = locals()[var_name]
    if 'depth' in var.dims:
        locals()[var_name] = var.isel(depth=0)

# === Match time to SST as a reference ===
uo = uo.interp_like(sst, method="nearest")
vo = vo.interp_like(sst, method="nearest")
sal = sal.interp_like(sst, method="nearest")
nit = nit.interp_like(sst, method="nearest")

# Interpolasi batimetri to SST grid
bati_interp = bati.interp_like(sst.isel(time=0), method="nearest").squeeze()

# Buat folder output
output_folder = "D:/RL/output_potensi_budidaya_2016"
os.makedirs(output_folder, exist_ok=True)

# === Loop for June-September ===
for bulan in [6, 7, 8, 9]:
    print(f"▶ Memproses bulan {bulan}...")

    # Take monthly data and average it
    sst_bln = sst.sel(time=sst['time.month'] == bulan).mean('time')
    sal_bln = sal.sel(time=sal['time.month'] == bulan).mean('time')
    nit_bln = nit.sel(time=nit['time.month'] == bulan).mean('time')
    u_bln = uo.sel(time=uo['time.month'] == bulan).mean('time')
    v_bln = vo.sel(time=vo['time.month'] == bulan).mean('time')

    # Current speed
    speed = np.sqrt(u_bln**2 + v_bln**2)

    # === Masking according to criteria ===
```

```
mask_sst = ((sst_bln >= 26) & (sst_bln <= 33)).astype(int) mask_sal =
((sal_bln >= 25) & (sal_bln <= 35)).astype(int)
mask_nit = ((nit_bln >= 1.61) & (nit_bln <= 70.96)).astype(int)
mask_ars = ((speed >= 0.1) & (speed <= 0.4)).astype(int)
mask_bati = ((bati_interp <= -0.3) & (bati_interp >= -10)).astype(int)

# Final score
mask_final = (mask_sst + mask_sal + mask_nit + mask_ars + mask_bati) / 5.0

# Get the coordinate dimension name
lat_dim = 'lat' if 'lat' in mask_final.dims else 'latitude' lon_dim = 'lon'
if 'lon' in mask_final.dims else 'longitude'

# If there are additional dimensions, the average
dims_to_reduce = [d for d in mask_final.dims if d not in [lat_dim, lon_dim]]
if dims_to_reduce:
    mask_2d = mask_final.mean(dim=dims_to_reduce)
else:
    mask_2d = mask_final

# Gaussian smoothing
smoothed_values = gaussian_filter(mask_2d.values, sigma=1)
mask_smooth = xr.DataArray(
    smoothed_values,
    coords={lat_dim: mask_2d[lat_dim], lon_dim: mask_2d[lon_dim]},
    dims=(lat_dim, lon_dim)
)
```

```
# === Focus to Cilacap & Kebumen ===
lat_min, lat_max = -8.0, -7.3
lon_min, lon_max = 108.5, 109.8
mask_smooth_cropped = mask_smooth.sel(
    {lat_dim: slice(lat_min, lat_max), lon_dim: slice(lon_min, lon_max)}
)

# === Plot ===
fig = plt.figure(figsize=(10, 4))
ax = plt.axes(projection=ccrs.PlateCarree()) im
= mask_smooth_cropped.plot(
    ax=ax,
    transform=ccrs.PlateCarree(), cmap='turbo',
    vmin=0,
    vmax=1,
    add_colorbar=True,
    cbar_kwargs={'label': 'Suitability Score (0–1)'}
)
ax.set_extent([lon_min, lon_max, lat_min, lat_max], crs=ccrs.PlateCarree())
ax.coastlines(resolution='10m', linewidth=1.5)
ax.add_feature(cfeature.BORDERS, linestyle=':')
ax.add_feature(cfeature.LAND, facecolor='lightgrey', edgecolor='black', zord
ax.set_title(f"Seaweed Cultivation Suitability – Cilacap & Kebumen – 2016 Mo
ax.gridlines(draw_labels=True, linestyle='--', alpha=0.5)
plt.tight_layout()
output_path = os.path.join(output_folder, f"potensi_budidaya_cilacap_kebumen
plt.savefig(output_path, dpi=300, bbox_inches='tight')
print(f"✓ Disimpan: {output_path}")
plt.close()
```

Supplementary Material Sensitivity Analysis Syntax

In [1]:

```
# ============================================================
# HSI Sensitivity Analysis
# Cilacap – Kebumen Coastal Waters
# Indian Ocean Dipole (IOD) Climate Conditions
# ============================================================

import xarray as xr
import numpy as np
import matplotlib.pyplot as plt
import cartopy.crs as ccrs
import cartopy.feature as cfeature import
matplotlib.ticker as mticker import os
=       ========================================
=       ====== # DATA DIRECTORY
=       #
=       ========================================================
=       =====
=
=       data_path = r"D:\RL\sensivitas"
=
=       # Climate conditions
=       climate_conditions = {
=           "Negative IOD": ("2016","IOD_negatif"),
=           "Neutral IOD": ("2018","IOD_normal"),
=           "Positive IOD": ("2019","IOD_positif")
=       }

        # Model parameters removed in sensitivity test
        parameters = ["sst","sss","nit","ars","bati"]

        # Parameter display names
        parameter_labels = {
            "sst":"SST",
            "sss":"SSS",
            "nit":"Nitrate",
            "ars":"Current Velocity",
            "bati":"Bathymetry"
        }
```

```
#
=======================================
==================== # REGION OF INTEREST
# Cilacap – Kebumen Coastal Area
#
=========================================================
=====

lat_min, lat_max = -8.0, -7.3
lon_min, lon_max = 108.5, 109.8

#
=======================================
==================== # LOAD NETCDF FUNCTION
#
=========================================================
=====

def load_hsi(year, parameter, condition):

    if parameter == "full":
        file = f"HSI_{year}_{condition}_full.nc"
    else:
        file = f"HSI_{year}_{condition}_no_{parameter}.nc"
```

```
    path = os.path.join(data_path,file)

    if not os.path.exists(path):
        print("Warning: File not found ->", path)

    return xr.open_dataset(path)

#
========================================
=================== # CALCULATE PARAMETER
SENSITIVITY
#
==================================================
=====

sensitivity_maps = {}
contribution_stats = {}

for condition,(year,cond_tag) in climate_conditions.items():
    ds_full = load_hsi(year,"full",cond_tag)
    HSI_full = ds_full.HSI.sel(
        latitude=slice(lat_min,lat_max),
        longitude=slice(lon_min,lon_max)
    )

    contribution_stats[condition] = {}
```

```
    for p in parameters:
        ds_ex = load_hsi(year,p,cond_tag)
        HSI_ex = ds_ex.HSI.sel(
            latitude=slice(lat_min,lat_max),
            longitude=slice(lon_min,lon_max)
        )

        # Sensitivity difference
        diff = abs(HSI_full - HSI_ex)

        sensitivity_maps[(condition,p)] = diff

        # Relative contribution
        contribution = diff / HSI_full
        contribution = contribution.where(np.isfinite(contribution))
        contribution_stats[condition][p] = float(contribution.mean())
#
=====================================
================== # MAP CONFIGURATION
#
=================================================
=====

lon = HSI_full.longitude lat
= HSI_full.latitude

vmin = 0
vmax = 0.5
#
=====================================
================== # PLOT SENSITIVITY MAPS
#
=================================================
=====

fig = plt.figure(figsize=(14,6))
```

```
proj = ccrs.PlateCarree() i =
1
for condition,(year,cond_tag) in climate_conditions.items():

    for p in parameters:

        ax = plt.subplot(3,5,i,projection=proj)
        data = sensitivity_maps[(condition,p)].mean("time")
        ax.add_feature(
            cfeature.LAND,
            facecolor='lightgray',
            edgecolor='black',
            linewidth=0.4,
            zorder=3
        )

        im = ax.pcolormesh(
            lon,
            lat, data,
            cmap="turbo",
            vmin=vmin,
            vmax=vmax,
            shading="auto",
            transform=proj
        )

        ax.add_feature(
```

```
        cfeature.COASTLINE,
        linewidth=0.6
)
ax.set_extent([lon_min,lon_max,lat_min,lat_max]) gl
= ax.gridlines(
        draw_labels=True,
        linewidth=0.25,
        linestyle="--",
        alpha=0.5
)

gl.top_labels = False
gl.right_labels = False

gl.xlocator = mticker.FixedLocator(np.arange(108.5,110,0.5)) gl.ylocator =
mticker.FixedLocator(np.arange(-8.0,-7.0,0.3))

gl.xlabel_style={'size':6}
gl.ylabel_style={'size':6}

ax.set_title(
        f"{condition} (Without {parameter_labels[p]})",
        fontsize=9
)
```

```
            i +=1


#
========================================
==================== # COLORBAR
#
============================================================
=====


cbar = fig.colorbar(
    im,
    ax=fig.axes,
    orientation="horizontal",
    fraction=0.05,
    pad=0.08
)


cbar.set_label(
"HSI Sensitivity Difference",
fontsize=11
)


#
======================================
==================== # LAYOUT ADJUSTMENT
#
========================================================
=====
```

```
plt.subplots_adjust(
left=0.06,
right=0.96, top=0.95,
bottom=0.2,
wspace=0.15,
hspace=0.15
)

plt.savefig(
    os.path.join(data_path,"HSI_Sensitivity_IOD_Cilacap_Kebumen.png"),
    dpi=600,
    bbox_inches="tight"
)

plt.show()

#
======================================
================== # PARAMETER
CONTRIBUTION BAR CHART
#
=========================================================
=====
labels = [parameter_labels[p] for p in parameters] x =
np.arange(len(labels))
width = 0.25
fig,ax = plt.subplots(figsize=(9,5))

for i,(condition,(year,cond_tag)) in enumerate(climate_conditions.items()): values =
    [contribution_stats[condition][p] for p in parameters]
    ax.bar(
        x + i*width,
        values,
        width,
        label=condition
```

```
        )

ax.set_xticks(x + width) ax.set_xticklabels(labels)

ax.set_ylabel("Relative Contribution to HSI") ax.set_title(
"Environmental Parameter Sensitivity of the Habitat Suitability Index (HSI)"
)

ax.legend()

plt.grid(alpha=0.3) plt.tight_layout()

plt.savefig(
        os.path.join(data_path,"HSI_Parameter_Contribution_IOD.png"), dpi=600
)

plt.show()

#
================================================
========= # PRINT SUMMARY
#  ============================================================

print("\nSensitivity Analysis of Environmental Parameters on the Habitat Suitabi

for condition in climate_conditions:

        print("Climate Condition:", condition)

        for p in parameters: print(
                        f"{parameter_labels[p]} contribution:", round(contribution_stats[condition][p],3)
                )

        print("")
```

Sensitivity Analysis of Environmental Parameters on the Habitat Suitability Index (HSI)

Climate Condition:
Negative IOD SST
contribution: 0.222
SSS contribution: 0.205
Nitrate contribution: 0.25
Current Velocity contribution: 0.145
Bathymetry contribution: 0.298

Climate Condition:
Neutral IOD SST contribution: 0.236
SSS contribution: 0.288
Nitrate contribution: 0.22
Current Velocity contribution: 0.246
Bathymetry contribution: 0.3

Climate Condition: Positive
IOD SST contribution: 0.26
SSS contribution: 0.311
Nitrate contribution: 0.206
Current Velocity contribution: 0.278
Bathymetry contribution: 0.301

In [ ]: